Synthesis, Structure, Spectroscopy, and Reactivity of a Metallabenzene[1]

John R. Bleeke,* Robert Behm, Yun-Feng Xie, Michael Y. Chiang, Kerry D. Robinson, and Alicia M. Beatty

Department of Chemistry, Washington University, St. Louis, Missouri 63130

Received December 3, 1996[⊗]

A rare example of a stable metallabenzene complex has been synthesized in three high-yield steps from (Cl)Ir(PEt_3)$_3$. In the first step, (Cl)Ir(PEt_3)$_3$ is treated with potassium 2,4-dimethylpentadienide to produce the metallacyclohexadiene complex *mer*-CH=C(Me)-CH=C(Me)CH_2Ir(PEt_3)$_3$(H) (**1b**) via metal-centered C−H bond activation. Treatment of **1b** with methyl trifluoromethanesulfonate removes the hydride ligand, producing [CH=C(Me)CH=C(Me)CH_2Ir(PEt_3)$_3$]$^+O_3SCF_3^-$ (**2**). Finally, deprotonation of **2** with base yields the metallabenzene complex CH=C(Me)CH=C(Me)CH=Ir(PEt_3)$_3$ (**3**). The X-ray crystal structure of **3** shows the coordination geometry about iridium to be square pyramidal. The metallabenzene ring is nearly planar, and the ring π-bonding is delocalized. In the ^{1}H NMR spectrum of **3**, the ring protons (H1/H5 and H3) are shifted downfield, consistent with the presence of an aromatic ring current. Compound **3** reacts with a variety of small 2e$^-$ ligands under mild conditions to produce monosubstituted metallabenzenes, CH=C(Me)-CH=C(Me)CH=Ir(PEt_3)$_2$L (**4a**, L = PMe_3; **4b**, L = $P(OMe)_3$; **4c**, L = CO), in which the unique ligand L resides preferentially in a basal coordination site. Under more forcing conditions, additional PEt_3 ligand replacements are observed. For example, treatment of **3** with 2 equiv of PMe_3 or $P(OMe)_3$ in toluene under reflux produces CH=C(Me)CH=C(Me)CH=Ir(PEt_3)L_2 (**5a**, L = PMe_3; **5b**, L = $P(OMe)_3$). Treatment of **3** with excess PMe_3 in toluene under reflux produces the tris-PMe_3 substitution product (**6**), while similar treatment with excess CO leads to carbonyl insertion and C−C coupling, ultimately yielding (3,5-dimethylphenoxy)-Ir(PEt_3)$_2$(CO) (**7**). Treatment of compound **3** with I_2, Br_2, or Ag^+/NCMe results in oxidation, and the production of octahedral Ir(III) complexes (**8a**, **8b**, and **9**, respectively) in which the metallabenzene ring is retained. Compound **3** undergoes 4 + 2 cycloaddition reactions with electron-poor substrates, including O_2, nitrosobenzene, maleic anhydride, CS_2, and SO_2. In each case, the cycloaddition substrate adds across iridium and C3 of the metallabenzene ring, producing octahedral products (**10**−**14**, respectively) with boat- shaped 1-iridacyclohexa-2,5-diene rings. In contrast, treatment of **3** with CO_2 leads to a 2 + 2 cycloaddition reaction in which the substrate adds across the Ir-C5 bond. The resulting octahedral adduct (**15**) contains a 1-iridacyclohexa-2,4-diene ring in a half-boat conformation. Finally, treatment of **3** with N_2O results in ring contraction and production of an iridacyclopentadiene species (**16**). Compound **3** reacts with electrophiles at the electron-rich α ring carbons, C1/C5. Hence, treatment with 1 equiv of $H^+O_3SCF_3^-$ regenerates compound **2**, while treatment with 2 equiv of $H^+O_3SCF_3^-$ produces [(η^5-2,4-dimethylpentadienyl)Ir(PEt_3)$_3$]$^{2+}$($O_3SCF_3^-$)$_2$ (**19**). Treatment of **3** with excess BF_3 leads to the production of a novel (η^6-borabenzene)iridium complex (**20**). This reaction apparently involves initial attack of BF_3 at ring carbon C5, followed by migration of ring carbon C1 to boron. Compound **3** displaces *p*-xylene from (*p*-xylene)-Mo(CO)$_3$ in tetrahydrofuran, generating the (η^6-metallabenzene)metal complex [η^6-CH=C-(Me)CH=C(Me)CH=Ir(PEt_3)$_3$]Mo(CO)$_3$ (**21**).

Introduction

"Aromaticity" has fascinated chemists ever since Kekulé[2] introduced the term to describe the unique properties of benzene. Of course, it is now well-established that a large family of benzenoid hydrocarbons exhibits "aromatic" properties, including high thermodynamic stability, delocalization of π bonds, and diamagnetic ring currents (diatropicity).[3] Furthermore, formal replacement of a benzene CH group with an isoelectronic heteroatom (N, P, As, O^+, S^+) leads to heterocyclic compounds in which aromaticity is retained.[4] While these so-called "heterobenzenes" have been thoroughly studied, comparatively little is known

[⊗] Abstract published in *Advance ACS Abstracts,* February 1, 1997.

S0276-7333(96)01012-6 CCC: $14.00

about the analogous compounds in which a transition-metal−ligand moiety replaces a benzene CH group. Particularly intriguing is the issue of whether (or to what extent) such "metallabenzenes" would exhibit aromatic physical and chemical properties.

Background

The first (and, prior to our work, only) example of a stable metallabenzene, $\overline{CH{=}CHCH{=}CHC(S){=}}Os(CO)(PPh_3)_2$ (see **A**, Figure 1), was reported by Roper and co-workers in 1982.[5] This complex was prepared via a cyclotrimerization reaction involving acetylene and the osmium thiocarbonyl complex $Os(CS)(CO)(PPh_3)_3$. Its X-ray crystal structure revealed a planar six-membered ring with no significant alternation in C−C bond lengths, supporting the idea of electron delocalization within the ring. Furthermore, low-field chemical shift values for the ring protons were observed in the ^{1}H NMR spectrum, providing additional evidence for aromaticity.[6] Very recently, Jones and Allison[7] have reported the low-temperature NMR detection of a ruthenabenzene (**B**, Figure 1), produced by intramolecular attack of a butadienyllithium ligand on a bound carbonyl. However, at −30 °C, this complex cleanly rearranges to a (η^3-cyclopentadienyl)ruthenium species by carbene migratory insertion.[8]

Several examples of *metal-coordinated* metallabenzenes have also been reported. Ernst has prepared a (η^6-molybdabenzene)metal complex (**C**, Figure 1) from the reaction of 2 equiv of (η^5-2,4-dimethylpentadienyl)-$Mo(CO)_3$ with ICH_2CH_2I.[9] Salzer has produced η^6-coordinated ruthenabenzene[10] (**D**, Figure 1) and nickelabenzene[11] (**E**, Figure 1) complexes by reacting (η^5-2,4-dimethylpentadienyl)RuCp* with appropriate

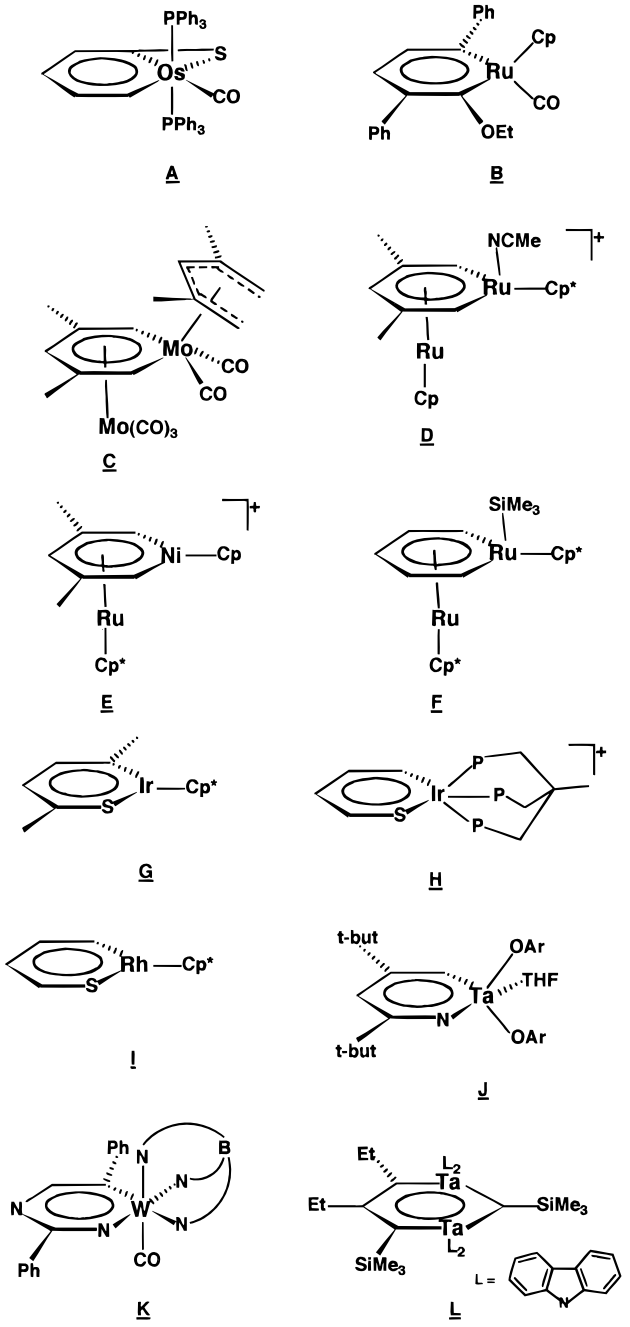

Figure 1. Literature examples of metallabenzenes, metal-coordinated metallabenzenes, and metallaheterobenzenes. References may be found in the text.

(cyclopentadienyl)ruthenium and (cyclopentadienyl)-nickel fragments. The intermediates in these reactions appear to be triple-decker complexes with a central pentadienyl ligand. Finally, Girolami[12] has reported the synthesis of a (η^6-ruthenabenzene)metal complex (**F**, Figure 1) from the reaction of acetylene with a methylene-bridged ruthenium dimer. This complex bears a strong structural similarity to Salzer's η^6-ruthenabenzene complex.

Several other related molecules are worthy of mention. Angelici[13] and Bianchini[14] have independently synthesized irida*thia*benzenes (**G** and **H**, Figure 1) via

(1) Metallacyclohexadiene and Metallabenzene Chemistry. 11. For previous papers in this series, see: (a) Bleeke, J. R.; Peng, W.-J. *Organometallics* **1987**, *6*, 1576. (b) Bleeke, J. R.; Xie, Y.-F.; Peng, W.-J.; Chiang, M. *J. Am. Chem. Soc.* **1989**, *111*, 4118. (c) Bleeke, J. R.; Peng, W.-J.; Xie, Y.-F.; Chiang, M. Y. *Organometallics* **1990**, *9*, 1113. (d) Bleeke, J. R.; Haile, T.; Chiang, M. Y. *Organometallics* **1991**, *10*, 19. (e) Bleeke, J. R.; Xie, Y.-F.; Bass, L.; Chiang, M. Y. *J. Am. Chem. Soc.* **1991**, *113*, 4703. (f) Bleeke, J. R.; Bass, L. A.; Xie, Y.-F.; Chiang, M. Y. *J. Am. Chem. Soc.* **1992**, *114*, 4213. (g) Bleeke, J. R.; Ortwerth, M. F.; Chiang, M. Y. *Organometallics* **1992**, *11*, 2740. (h) Bleeke, J. R.; Haile, T.; New, P. R.; Chiang, M. Y. *Organometallics* **1993**, *12*, 517. (i) Bleeke, J. R.; Rohde, A. M.; Boorsma, D. W. *Organometallics* **1993**, *12*, 970. (j) Bleeke, J. R.; Behm, R.; Xie, Y.-F.; Clayton, T. W., Jr.; Robinson, K. D. *J. Am. Chem. Soc.* **1994**, *116*, 4093. See also: Bleeke, J. R. *Acc. Chem. Res.* **1991**, *24*, 271.

(2) (a) Kekulé, A. *Bull. Soc. Chim. Paris* **1865**, (ii)*3*, 98. (b) Kekulé, A. *Bull. Acad. R. Belg.* **1865**, *19*, 551.

(3) (a) Badger, G. M. *Aromatic Character and Aromaticity;* Cambridge University Press: London, 1969. (b) Garratt, P. J. *Aromaticity;* McGraw-Hill: London, 1971. (c) Bergmann, E. D., Pullman, B., Eds. *Aromaticity, Pseudo-Aromaticity, Anti-Aromaticity;* Academic Press: New York, 1971. (d) March, J. *Advanced Organic Chemistry,* 3rd ed.; Wiley: New York, 1985; pp 37−64.

(4) (a) Ashe, A. J., III. *Acc. Chem. Res.* **1978**, *11*, 153. (b) Jutzi, P. *Angew. Chem., Int. Ed. Engl.* **1975**, *14*, 232.

(5) Elliott, G. P.; Roper, W. R.; Waters, J. M. *J. Chem. Soc., Chem. Commun.* **1982**, 811.

(6) Elliott, G. P.; McAuley, N. M.; Roper, W. R. *Inorg. Synth.* **1989**, *26*, 184.

(7) Yang, J.; Jones, W. M.; Dixon, J. K.; Allison, N. *J. Am. Chem. Soc.* **1995**, *117*, 9776.

(8) Metallabenzenes have also been postulated as possible intermediates in several related reactions studies by Allison. See: (a) Ferede, R.; Allison, N. T. *Organometallics* **1983**, *2*, 463. (b) Ferede, R.; Hinton, J. F.; Korfmacher, W. A.; Freeman, J. P.; Allison, N. T. *Organometallics* **1985**, *4*, 614. (c) Mike, C. A.; Ferede, R.; Allison, N. T. *Organometallics* **1988**, *7*, 1457.

(9) Kralik, M. S.; Rheingold, A. L.; Ernst, R. D. *Organometallics* **1987**, *6*, 2612.

(10) Bosch, H. W.; Hund, H.-U.; Nietlispach, D.; Salzer, A. *Organometallics* **1992**, *11*, 2087.

(11) Bertling, U.; Englert, U.; Salzer, A. *Angew. Chem., Int. Ed. Engl.* **1994**, *33*, 1003.

(12) Lin, W.; Wilson, S. R.; Girolami, G. *J. Chem. Soc., Chem. Commun.* **1993**, 284.

(13) Chen, J.; Daniels, L. M.; Angelici, R. J. *J. Am. Chem. Soc.* **1990**, *112*, 199.

Scheme 1

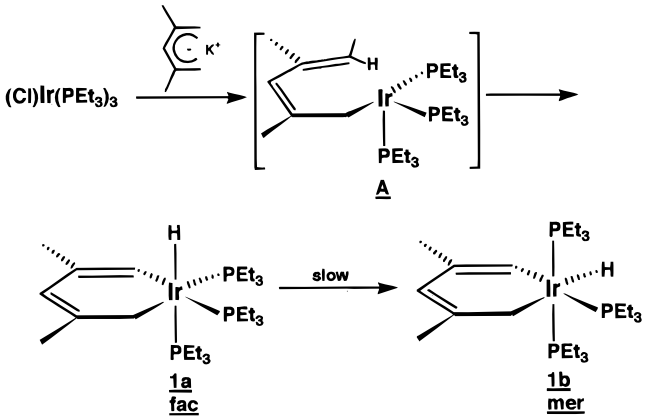

Scheme 2

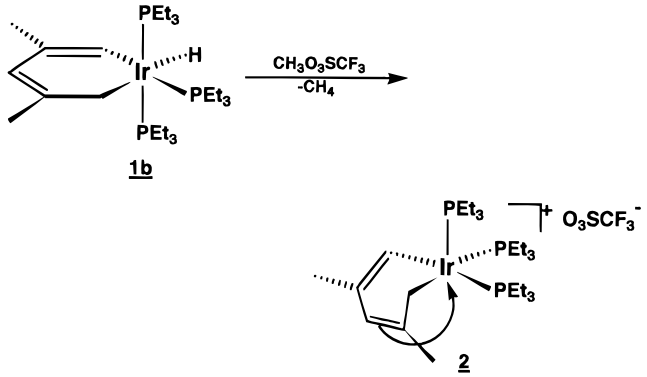

insertion of iridium into C—S bonds of thiophene. The unmethylated rhodium analogue of **G** (I, Figure 1) has likewise been generated in a thiophene ring-opening reaction but is thermally unstable.[15] A tantalapyridine complex (**J**) has been reported by Wigley,[16] while tungstapyrimidine species (**K**) have been synthesized by Templeton.[17] Finally, a family of 1,3-*dimetalla*benzenes, generated by alkyne insertion into dimetallacyclobutadienes (**L**), have been reported by Rothwell.[18]

Results and Discussion

A. Synthesis of an "Iridabenzene", CH=C(Me)-CH=C(Me)CH=Ir(PEt$_3$)$_3$ (3). Our work in the area of metallabenzene chemistry dates back to the late 1980s, when we discovered that treatment of (Cl)Ir(PEt$_3$)$_3$ with potassium 2,4-dimethylpentadienide in tetrahydrofuran produces the metallacyclohexadiene complex CH=C(Me)CH=C(Me)CH$_2$Ir(PEt$_3$)$_3$(H) (**1**) in high yield.[1a] The kinetic product of this reaction is the *fac* isomer (**1a**), which slowly isomerizes to the more thermodynamically favorable *mer* isomer (**1b**) over the course of 24 h at 25 °C. The probable mechanism of this reaction, shown in Scheme 1, involves the intermediacy of the 16e$^-$ species (η^1-2,4-dimethylpentadienyl)Ir(PEt$_3$)$_3$ (**A**), which undergoes intramolecular oxidative addition across an sp^2 C—H bond on the dangling terminus of the η^1-pentadienyl ligand. The crystal structure of **1b**, reported earlier,[1a] shows the metallacyclic ring to be essentially planar. This planarity is also manifested in the solution-phase NMR spectra of **1b**. Hence, the two protons bonded to C5 (the sp^3 carbon) are equivalent and give rise to a single peak in the ^{1}H NMR spectrum. Similarly, the two mutually *trans* phosphines are equivalent by ^{1}H, ^{13}C, and ^{31}P NMR spectroscopy.

As shown in Scheme 2, treatment of **1b** with methyl trifluoromethanesulfonate results in abstraction of the hydride ligand[19] and coordination of the ring double bond C3—C4 to the iridium center, generating the (1,3,4,5-η)-pentadienediyl complex [CH=C(Me)CH=C(Me)CH$_2$Ir(PEt$_3$)$_3$]$^+$O$_3$SCF$_3^-$ (**2**). The crystal structure of **2**, reported earlier,[1a] shows a rather weak, strained interaction between the ring double bond and the iridium atom. In solution, compound **2** exhibits fluxional behavior. At −80 °C, the ^{31}P{^{1}H} NMR spectrum consists of three sharp doublet-of-doublets patterns, due to the three inequivalent PEt$_3$ ligands. When the temperature is raised, however, these peaks broaden and ultimately coalesce at about 20 °C. In the ^{1}H NMR spectrum, separate peaks due to H1 and the two H5's are well-resolved at −80 °C, but when the temperature is raised, these peaks broaden and coalesce at about 10 °C. Similarly, the signals for the two ring methyl groups broaden and coalesce. Analysis of the variable-temperature ^{31}P and ^{1}H NMR line shapes yields a free energy of activation ($\Delta G^{\ddagger}$) of 12.8 ± 0.2 kcal/mol for each of these processes, which we believe involve the 16e$^-$ "unhinged" metallacyclohexadiene complex (**B**, Scheme 3) as the key intermediate. In this five-coordinate species, phosphine ligand exchange is expected to be facile. Furthermore, exchange of the ring α-hydrogens (H1 and the two H5's) could be metal-mediated, proceeding through a transient 18e$^-$ metallabenzene−hydride intermediate (**C**, Scheme 3).[20,21] This exchange process would, of course, also cause the ring methyl groups to become equivalent.

Compound **2** is stable indefinitely in the solid state and in solution at −30 °C but slowly (over the course of several days) decomposes to [(η^5-1,3-dimethylcyclopentadienyl)Ir(PEt$_3$)$_2$(H)]$^+$O$_3$SCF$_3^-$ when it is warmed to 25 °C in solution. We propose that this reaction proceeds via initial loss of PEt$_3$ to produce 16e$^-$ [CH=C(Me)CH=C(Me)CH$_2$Ir(PEt$_3$)$_2$]$^+$O$_3$SCF$_3^-$ (**D**, Scheme 4). This species then undergoes C—C bond formation, generating 16e$^-$ [(η^4-1,3-dimethylcyclo-

(14) (a) Bianchini, C.; Meli, A.; Peruzzini, M.; Vizza, F.; Frediani, P.; Herrera, V.; Sanchez-Delgado, R. A. *J. Am. Chem. Soc.* **1993**, *115*, 2731. (b) Bianchini, C.; Meli, A.; Peruzzini, M.; Vizza, F.; Moneti, S.; Herrera, V.; Sanchez-Delgado, R. A. *J. Am. Chem. Soc.* **1994**, *116*, 4370.

(15) Chin, R. M.; Jones, W. D. *Angew. Chem., Int. Ed. Engl.* **1992**, *31*, 357.

(16) Wigley, D. E. Division of Inorganic Chemistry, 211th National Meeting of the American Chemical Society, New Orleans, LA, March 1996.

(17) Feng, S. G.; White, P. S.; Templeton, J. L. *Organometallics* **1993**, *12*, 1765.

(18) Profilet, R. D.; Fanwick, P. E.; Rothwell, I. P. *Angew. Chem., Int. Ed. Engl.* **1992**, *31*, 1261.

(19) Methane is detected as a product of the reaction by gas chromatography.

(20) Reversible hydrogen migration from α-carbon to iridium is known: (a) Fryzuk, M. D.; MacNeil, P. A.; Rettig, S. J. *J. Am. Chem. Soc.* **1985**, *107*, 6708. (b) Crocker, C.; Empsall, H. D.; Errington, R. J.; Hyde, E. M.; McDonald, W. S.; Markham, R.; Norton, M. C.; Shaw, R. L.; Weeks, B. *J. Chem. Soc., Dalton Trans.* **1982**, 1217. (c) Burk, M. J.; McGrath, M. P.; Crabtree, R. H. *J. Am. Chem. Soc.* **1988**, *110*, 620.

(21) Hughes has also proposed an iridabenzene intermediate to explain phenyl group migration between the α-carbons of an iridacyclohexadiene ring: Hughes, R. P.; Trujillo, H. A.; Rheingold, A. L. *J. Am. Chem. Soc.* **1993**, *115*, 1583.

Scheme 3

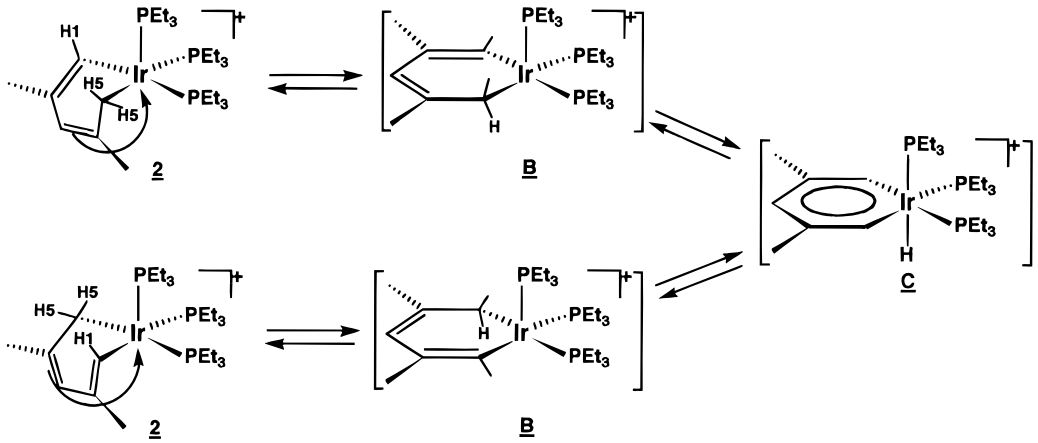

Scheme 4

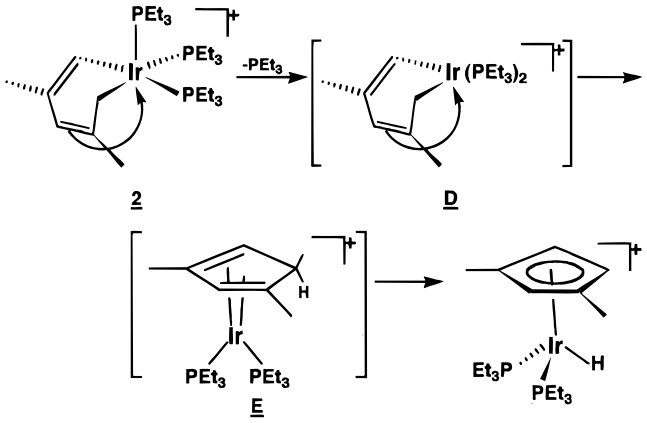

Scheme 5

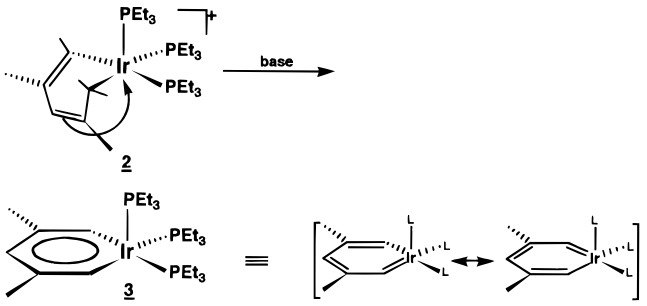

pentadiene)Ir(PEt_3)$_2$]$^+O_3SCF_3^-$ (**E**, Scheme 4).[22] Finally, endo-H abstraction by the iridium center yields the observed 18e$^-$ product [(η^5-1,3-dimethylcyclopentadienyl)Ir(PEt_3)$_2$(H)]$^+O_3SCF_3^-$.

Treatment of compound **2** with acetone enolate (generated *in situ* from acetone and lithium diisopropylamide) at −30 °C results in proton abstraction and production of "iridabenzene", CH=C(Me)CH=C(Me)-CH=Ir(PEt_3)$_3$ (**3**, Scheme 5).[1b] Compound **3** is also produced upon treatment of **2** with sodium hydroxide in tetrahydrofuran. Although the mechanistic details of the deprotonation reaction are not known, it seems likely that the 16e$^-$ "unhinged" metallacyclohexadiene complex (**B**, Scheme 3) is involved. As discussed above, this species also appears to be the key intermediate responsible for the fluxional behavior of **2** and may be in equilibrium with the transient metallabenzene−hydride species **C**. Hence, the deprotonation of **2** could occur directly from unhinged iridacyclohexadiene **B**, from iridabenzene−hydride **C**, or even from an agostic species on the pathway from **B** to **C**.

B. Structure and Spectroscopy of Iridabenzene

3. The solid-state structure of CH=C(Me)CH=C(Me)-CH=Ir(PEt_3)$_3$ (**3**), determined by single-crystal X-ray diffraction, is shown in Figure 2;[23] selected bond distances and angles are given in the figure caption. The coordination geometry is square pyramidal, with C1, C5, P1, and P2 occupying the four basal sites and P3 residing in the axial site. The carbon portion of the metallacyclic ring (C1/C2/C3/C4/C5) is very nearly planar (mean deviation 0.014 Å), while the iridium center lies 0.24 Å out of this plane. The dihedral angle between planes C1/C2/C3/C4/C5 and C1/Ir/C5 is 9.2°. The displacement of the iridium center from the ring plane probably results—at least in part—from steric interactions involving the basal phosphine ligands and the ring. Bonding within the ring is highly delocalized, and the bond lengths (C1−C2 = 1.37(1) Å, C2−C3 = 1.40(1) Å, C3−C4 = 1.37(1) Å, C4−C5 = 1.39(1) Å) are comparable to those found in benzene itself (1.398(9) Å).[24] The iridium−carbon distances (Ir−C1 = 2.024(8) Å, Ir−C5 = 1.985(8) Å) are, as expected, intermediate between normal Ir−C single[25] and double[26] bonds (2.11 and 1.87 Å, respectively). The bond angles within the carbon portion of the ring are 122.6(7)° (C1−C2−C3), 125.3(7)° (C2−C3−C4), and 121.8(7)° (C3−C4−C5), while the Ir−C1−C2 and C4−C5−Ir angles are 131.2(6) and 132.9(6)°, respectively, and the C1−Ir−C5 angle is 84.7(3)°.[27]

(22) Detailed mechanistic studies of a closely related reaction involving the (1,3,4,5-η)-pentadienediyl complex C(*t*-Bu)=C(*t*-Bu)C(*t*-Bu)=CHCH$_2$Rh(indenyl) have established that ring closure involves direct C−C bond formation across the puckered 1,3,4,5-η ligand. Metallacyclohexadiene and metallabenzene intermediates are excluded. See: Donovan, B. T.; Hughes, R. P.; Trujillo, H. A. *J. Am. Chem. Soc.* **1990**, *112*, 7076.

(23) A preliminary report of this structure has been communicated in ref 1b.

(24) Bacon, G. E.; Curry, N. A.; Wilson, S. A. *Proc. R. Soc. London, Ser. A* **1964**, *279*, 98.

(25) Orpen, A. G.; Brammer, L.; Allen, F. H.; Kennard, O.; Watson, D. G.; Taylor, R. *J. Chem. Soc., Dalton Trans.* **1989**, S1.

(26) (a) Clark, G. R.; Roper, W. R.; Wright, A. H. *J. Organomet. Chem.* **1982**, *236*, C7. (b) Fryzuk, M. D.; MacNeil, P. A.; Rettig, S. J. *J. Am. Chem. Soc.* **1985**, *107*, 6708.

(27) The relatively small C−Ir−C angle allows the long Ir−C bonds to be accommodated within a planar ring structure.

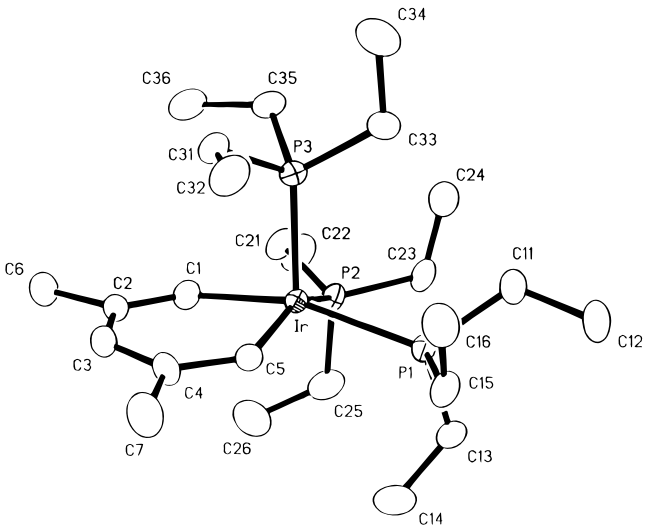

Figure 2. ORTEP drawing of CH═C(Me)CH═C(Me)-CH═Ir(PEt_3)$_3$ (**3**). Selected bond distances (Å) with estimated standard deviations: Ir−P1, 2.379(2); Ir−P2, 2.369(2); Ir−P3, 2.268(2); Ir−C1, 2.024(8); Ir−C5; 1.985(8); C1−C2, 1.369(10); C2−C3, 1.402(11); C2−C6, 1.523(11); C3−C4, 1.370(11); C4−C5, 1.392(10); C4−C7, 1.503(12). Selected bond angles (deg) with estimated standard deviations: P1−Ir−P2, 93.0(1); P1−Ir−P3, 105.0(1); P2−Ir−P3, 103.0(1); P1−Ir−C1, 163.8(2); P2−Ir−C1, 87.6(2); P3−Ir−C1, 90.6(2); P1−Ir−C5, 87.3(2); P2−Ir−C5, 152.2(2); P3−Ir−C5, 103.7(2); C1−Ir−C5, 84.7(3); Ir−C1−C2, 131.2(6); C1−C2−C3, 122.6(7); C1−C2−C6, 119.8(7); C3−C2−C6, 117.6(6); C2−C3−C4, 125.3(7); C3−C4−C5, 121.8(7); C3−C4−C7, 119.1(7); C5−C4−C7, 119.0(7); Ir−C5−C4, 132.9(6).

In the ^{1}H NMR spectrum of compound **3** in acetone-d_6, the signal for H1/H5 appears at δ 10.91, while H3 resonates at δ 7.18.[28] By comparsion, H1 and H3 of the metallacyclohexadiene precursor **1b** resonate at δ 7.00 and δ 5.93, respectively. The downfield shift of the H1/H5 protons in **3** reflects the carbenic nature of the C1/C5 carbons (these carbons have 50% carbene character, based on simple resonance pictures) and can be attributed primarily to the magnetic anisotropic influences of the large metal atom. However, such effects are strongly dependent on internuclear separation[29] and decrease rapidly for protons remote from the metal center. For example, in the recently reported ruthenium−vinylcarbene complex $(Cl)_2(PCy_3)_2Ru$═CHCH═CH_2, the chemical shifts of the protons along the vinylcarbene chain decrease from δ 19.06 for H_α to δ 8.11 for H_β to δ 6.25/6.01 for H_γ's.[30] Hence, we believe that the significant downfield chemical shift of H3 (δ 7.18) results mainly from the influence of an aromatic ring current rather than a metal-based anisotropy. The ^{13}C{^{1}H} NMR spectrum of **3** follows the trend seen in the ^{1}H NMR spectrum. Equivalent carbons C1 and C5 resonate quite far downfield at δ 167.6, while C2/C4 and C3 appear in the normal aromatic region, at δ 132.0 and δ 129.9, respectively.

The ^{31}P{^{1}H} NMR signal for **3** is a sharp singlet, which shows no broadening even when the sample is cooled to −80 °C. This indicates that **3** is stereochemically nonrigid and that the axial and basal phosphines

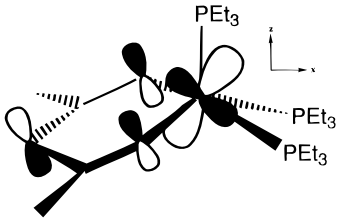

Figure 3. Key orbital interaction in "iridabenzene", involving a metal d orbital (d_{xz}/d_{z^2} hybrid) and the 3π orbital of the organic moiety. This orbital also serves as the effective HOMO for iridabenzene.

Scheme 6

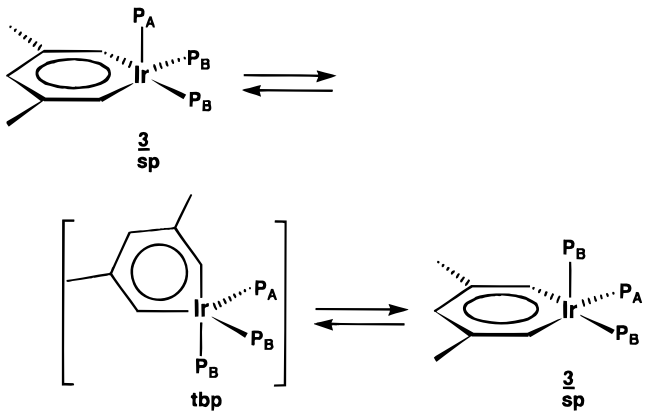

are exchanging rapidly in solution, probably via a Berry-type process.[31] In the Berry-type process (Scheme 6) the square-pyramidal complex isomerizes to a trigonal-bipyramidal intermediate (tbp) in which one ring carbon atom and one basal phosphine ligand (P_B) assume *trans*-diaxial positions. This intermediate then reisomerizes back to the square-pyramidal complex, causing P_A/P_B exchange. As a result of the phosphine exchange process, the H1/H5 signal in the ^{1}H NMR spectrum of **3** appears as a binomial quartet with J_{H-P} = 7.2 Hz. Likewise, the C1/C5 signal in the ^{13}C{^{1}H} NMR is a binomial quartet with J_{C-P} = 28.1 Hz.

C. Orbital Considerations. Thorn and Hoffmann were the first to carry out molecular orbital calculations on delocalized metallacycles such as metallabenzenes. In fact, in a prescient 1978 publication,[32] they predicted that square-pyramidal (metallabenzene)L_3 (M = Rh, Ir; L = electron-donating ligand) should be an unusually stable structure, exhibiting delocalization and aromatic character. The key to the stability of this structure was good overlap between a filled metal hybrid d_{xz}/d_{z^2} orbital and the empty 3π molecular orbital of the C_5H_5 carbon fragment (see Figure 3).[33] Of course, there were two additional filled carbon-based ring π orbitals (1π and 2π), bringing the total π-electron count to the magic Hückel number of 6.

Thorn and Hoffmann treated the C_5H_5 fragment in (metallabenzene)L_3 as a monoanionic ligand[34] and,

(28) In benzene-d_6, the peaks for H1/H5 and H3 are even more downfield, appearing at δ 11.20 and 7.80, respectively.
(29) McConnell, H. M. *J. Chem. Phys.* **1957**, *27*, 226.
(30) Schwab, P.; Grubbs, R. H.; Ziller, J. W. *J. Am. Chem. Soc.* **1996**, *118*, 100.
(31) (a) For a discussion of this process as applied to the trigonal-bipyramidal case, see: Cotton, F. A.; Wilkinson, G. *Advanced Inorganic Chemistry*, 4th ed.; Wiley: New York, 1980; pp 1218−1220. (b) Phosphine ligand dissociation occurs much too slowly, even at room temperature, to be involved in the fluxional process.
(32) Thorn, D. L.; Hoffmann, R. *Nouv. J. Chim.* **1979**, *3*, 39.
(33) The structure was further stabilized by a weak interaction between the filled metal d_{yz} orbital and the empty 4π* MO of the carbon fragment.
(34) In a localized valence bond picture, this is equivalent to counting the carbene moiety of the C_5H_5 fragment as a neutral 2e$^-$ (Fischer type) ligand.

Scheme 7

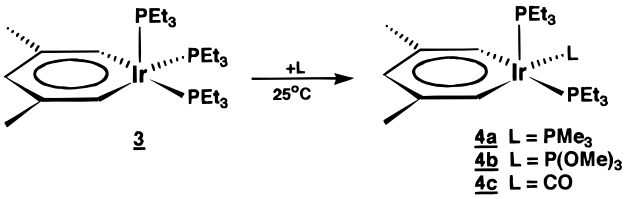

therefore, the metal as a M(I) ≡ d^8 center. In this view, the M−C π interaction results from back-bonding *from* the metal *to* the 3π orbital of the carbon ligand. An alternative approach is to treat the C_5H_5 fragment as a trianionic ligand.[35] In this case, 3π is filled and the metal is a M(III) ≡ d^6 center. Here, π electron flow is *from* the carbon ligand *to* the metal. These two bonding pictures are complementary, and each is supported by aspects of compound **3**'s reaction chemistry (*vide infra*).[36]

D. Chemical Reactivity of Iridabenzene 3. Although metallabenzenes have been implicated as intermediates in the formation of a variety of (cyclopentadienyl)metal complexes,[8,37] compound **3** is quite robust. In the solid state or in solution at room temperature (under an N_2 atmosphere) it is stable indefinitely. Decomposition does occur slowly in refluxing benzene, but this process can be significantly retarded by the addition of excess PEt_3, suggesting that phosphine dissociation precedes decomposition. While **3** shows good thermal stability, it is also highly reactive toward a wide range of substrates. This reactivity is described in detail in the sections that follow.

1. Ligand Substitution. Iridabenzene **3** undergoes ligand replacement reactions with a variety of small 2e⁻ ligands L, including PMe_3, $P(OMe)_3$, and CO, to produce species of formula $\overline{CH{=}C(Me)CH{=}C(Me)CH{=}}Ir(PEt_3)_2(L)$ (**4a**, L = PMe_3; **4b**, L = $P(OMe)_3$; **4c**, L = CO) (see Scheme 7). At room temperature, only *one* PEt_3 ligand is replaced, even when excess L is employed. In order to probe the mechanism of ligand replacement, a kinetic study of the reaction of **3** with PMe_3 was undertaken. The reaction was monitored by $^{31}P\{^1H\}$ NMR spectroscopy at 15, 25, and 35 °C. At each temperature, a plot of $\ln([\mathbf{3}]/[\mathbf{3}]_0)$ versus time yielded a straight line, indicating clean first-order kinetics. The rate constants (k), obtained from the slopes of the straight-line plots, were 2.0×10^{-5}, 1.1×10^{-4}, and 6.7×10^{-4} s^{-1} at 15, 25, and 35 °C, respectively. These rate constants were independent of PMe_3 reagent concentration. An "Eyring plot" of $\ln(k/T)$ versus $1/T$ yielded a straight line, from which values for $\Delta H^{\ddagger}$ (30 ± 3 kcal/mol) and $\Delta S^{\ddagger}$ (25 ± 3 cal/mol·K) could be obtained. These kinetic results are fully consistent with a dissociative mechanism, where loss of PEt_3 from **3** is the rate-limiting step.[38]

In solution, compounds **4a**−**c** exhibit *apparent* mirror-plane symmetry by NMR, even at −80 °C. Hence, H1 and H5 appear equivalent, C1 and C5 appear equivalent, and so on. The $^{31}P\{^1H\}$ NMR spectra of **4a**−**b**, consist of a doublet (PEt_3's) and a triplet (PMe_3 or $P(OMe)_3$), while the $^{31}P\{^1H\}$ NMR spectrum of **4c** is a sharp singlet. Several interpretations of these spectra are possible. First, the compounds could possess static symmetrical structures in which the unique ligand L resides in the unique axial coordination site of the square pyramid. Second, the compounds could be stereochemically nonrigid with the three ligands spending equal time in the three available coordination sites. Third, the compounds could be stereochemically nonrigid, with the unique ligand L spending a disproportionate fraction of its time in the basal or axial coordination sites. As described below, a careful analysis of P−H coupling constants in these molecules strongly supports the last of these possibilities, with L residing preferentially in the basal plane.

By studying H−P coupling constants in (η^6-iridabenzene)$Mo(CO)_3$ complexes (in which intramolecular ligand exchange is completely arrested),[1f] we have established that coupling between an α ring proton and the *cis* basal phosphine is large ($J_{H-P} \approx 20-30$ Hz), while coupling of H_α to the *trans* basal phosphine and axial phosphine is small ($J_{H-P} < 5$ Hz). Hence, the magnitude of H_α−P

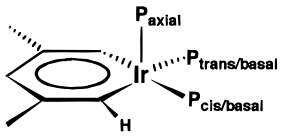

coupling constants provides information about the phosphine coordination geometry. We find that, in compound **4a**, the H1/H5 ^1H NMR signal is a doublet (J_{H-P} = 14.8 Hz) of triplets (J_{H-P} = 4.1 Hz) centered at δ 10.85. Selective ^{31}P decoupling of the PMe_3 signal causes the doublet coupling to disappear, while selective ^{31}P decoupling of the PEt_3 signal removes the triplet coupling. Hence, PMe_3 is responsible for the 14.8 Hz coupling while two rapidly exchanging PEt_3's are responsible for the 4.1 Hz coupling. From the magnitude of these numbers, it is clear that PMe_3 resides preferentially in the basal plane (and spends approximately half of its time *cis* to each α ring proton), while the PEt_3 ligands exchange between basal and axial sites (and spend approximately one-fourth of their time *cis* to each α ring proton). Similar analysis of H−P coupling constants in **4b**,**c** strongly suggests that they are isostructural with **4a**.[39]

The ligand site preferences in these compounds are easily rationalized on steric grounds. In square-pyramidal coordination complexes, the axial site is less congested than the basal site. For example, in the structure of **3**, the $P_{axial}-Ir-P_{basal}$ angles are 105.0 and 103.0°, while the $P_{basal}-Ir-P_{basal}$ angle is 93.0°. Hence, a bulky PEt_3 ligand resides preferentially in the roomier axial site.

While only one PEt_3 substitution is observed at room temperature, additional substitutions occur under more forcing conditions. Hence, when **3** is treated with 2 equiv of PMe_3 or $P(OMe)_3$ in toluene at reflux, the bis-PMe_3 and bis-$P(OMe)_3$ substitution products (**5a**,**b**, respectively) are formed (see Scheme 8). Like **4a**−**c**, compounds **5a**,**b** exhibit mirror-plane symmetry by NMR. Hence, H1 and H5 appear equivalent, C1 and

(35) In a localized valence bond picture, this is equivalent to counting the carbene moiety as a dianionic 4e⁻ (Schrock type) ligand.

(36) The bonding in iridabenzene has also been discussed briefly by Eisenstein et al. See: Bianchini, C.; Caulton, K. G.; Chardon, C.; Doublet, M.-L.; Eisenstein, O.; Jackson, S. A.; Johnson, T. J.; Meli, A.; Peruzzini, M.; Streib, W. E.; Vacca, A.; Vizza, F. *Organometallics* **1994**, *13*, 2010.

(37) Schrock, R. R.; Pedersen, S. F.; Churchill, M. R.; Ziller, J. W. *Organometallics* **1984**, *3*, 1574.

(38) Atwood, J. D. *Inorganic and Organometallic Reaction Mechanisms*; Brooks/Cole: Monterey, CA, 1985.

(39) The structure of **4b** has been confirmed by X-ray crystallography: Bleeke, J. R.; Xie, Y.-F.; Chiang, M. Y. Unpublished results.

Scheme 8

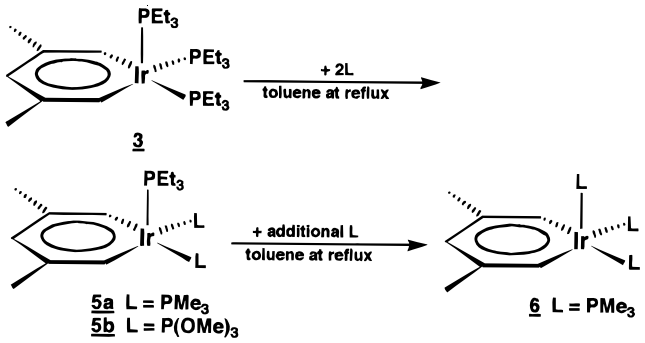

C5 appear equivalent, etc. Furthermore, the molecules are stereochemically nonrigid; therefore, the H1/H5 signal exhibits triplet coupling to the two exchanging PMe_3 or $P(OMe)_3$ ligands. The large size of this coupling (J = 12.6 Hz for **5a** and 8.9 Hz for **5b**) strongly suggests that the PMe_3 or $P(OMe)_3$ ligands reside preferentially in the basal plane, where coupling to H1/H5 is maximized. In contrast, coupling of H1/H5 to PEt_3 is small (unobservable in **5a**, 3.7 Hz in **5b**), confirming that the large PEt_3 ligand spends the majority of its time in the axial position.

As shown in Scheme 8, treatment of **3** with excess PMe_3 in toluene at reflux generates the tris-PMe_3 substitution product (**6**). In contrast, treatment of **3** with excess $P(OMe)_3$ under identical conditions yields only the bis-$P(OMe)_3$ substitution product **5b**. Hence, there appears to be a strong electronic preference for retaining at least one good σ-donor ligand in the iridabenzene coordination sphere.

The NMR spectra of compound **6** are virtually identical with those of **3**. The $^{31}P\{^1H\}$ NMR spectrum is a sharp singlet, due to rapidly exchanging PMe_3 ligands. The H1/H5 signal is a binomial quartet (J_{H-P} = 8.0 Hz) at δ 10.62, while H3 resonates at δ 7.10. Similarly, the C1/C5 signal is a binominal quartet (J_{C-P} = 30.1 Hz) at δ 167.9, while C2/C4 and C3 resonate at δ 133.1 and δ 129.1, respectively. Compound **6** is extremely robust, showing little or no decomposition in refluxing toluene.

The structure of **6** has been confirmed by X-ray crystallography (see Figure 4). The square-pyramidal molecule resides on a crystallographically imposed mirror plane containing Ir, ring carbon C3, and axial phosphorus P2. Bonding within the metallacyclic ring is fully delocalized; the Ir−C1, C1−C2, and C2−C3 distances are 2.008(7), 1.390(10), and 1.387(10) Å, respectively. Furthermore, the ring is even more planar than in compound **3**, probably as a result of reduced steric interactions with the basal phosphine ligands. The iridium center lies only 0.17 Å out of the plane of the ring carbon atoms (C1/C2/C3/C2a/C1a), while the dihedral angle between this plane and the C1/Ir/Cla plane is a mere 6.7°.

When compound **3** is treated with excess carbon monoxide in toluene at reflux, a novel rearrangement occurs, generating the iridium−phenoxide compound **7** (see Scheme 9).[40] Although the detailed mechanism of this reaction has not been established, it probably involves CO insertion into an iridabenzene Ir−C_α bond, followed by ring closure and metal migration to the oxygen center (Scheme 9).

(40) The structure of **7** has been confirmed by X-ray crystallography: Bleeke, J. R.; Behm, R.; Beatty, A. M. Unpublished results.

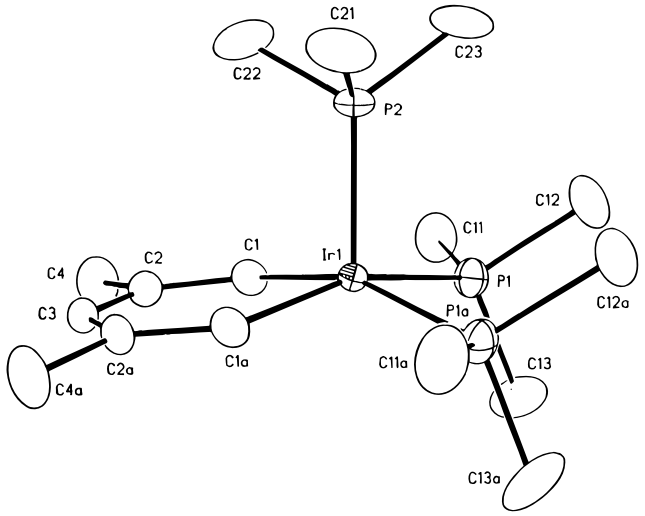

Figure 4. ORTEP drawing of CH=C(Me)CH=C(Me)-CH=Ir(PMe_3)$_3$ (**6**). Selected bond distances (Å) with estimated standard deviations: Ir−P1, 2.327(2); Ir−P2, 2.236(3); Ir−C1, 2.008(7); C1−C2, 1.390(10); C2−C3, 1.387(10); C2−C4, 1.528(11). Selected bond angles (deg) with estimated standard deviations: P1−Ir−P2, 99.05(8); P1−Ir−P1a, 94.43(11); P1−Ir−C1, 87.0(2); P1a−Ir−C1, 161.1(2); P2−Ir−C1, 99.3(2); C1−Ir−C1a, 85.7(4); Ir−C1−C2, 131.1(6); C1−C2−C3, 123.2(8); C1−C2−C4, 119.0(8); C2−C3−C2a, 124.9(10); C3−C2−C4, 117.7(7).

2. Oxidative Addition/Oxidation. Iridabenzene **3** reacts slowly with excess H_2 gas at room temperature and 1 atm of pressure to generate 2,4-dimethyl-1,3-pentadiene, 2,4-dimethyl-1-pentene, and iridium polyhydrides. The principal hydride product is $(H)_5Ir(PEt_3)_2$, with smaller quantities of *mer*- and *fac*-$(H)_3Ir(PEt_3)_3$ being observed.[41] One reasonable mechanism for this reaction, outlined in Scheme 10, involves dissociation of PEt_3 (**H**), oxidative addition of H_2 to the iridium center (**I**), and hydride migration from iridium to an α-carbon of the ring (**J**, **K**).[42] Further hydrogen addition and migration steps would lead ultimately to the observed organic and inorganic products. The rate of the hydrogenation reaction is drastically retarded by addition of excess PEt_3 to the reaction mixture, suggesting that the phosphine dissociation step is rate-limiting. Furthermore, compounds **4a**−**c** do not react with H_2 at 25 °C, presumably because the 16e$^-$ intermediates cannot be accessed in these cases.

Treatment of **3** with iodine (I_2) leads to very rapid production of the olive green oxidative addition product CH=C(Me)CH=C(Me)CH=Ir(PEt_3)$_2$(I)$_2$ (**8a**) (see Scheme 11).[1e] The rapid rate of this reaction suggests that initial phosphine ligand dissociation is *not* required. More likely, the initial step is rapid electron transfer from **3** to the iodine reagent.

The solid-state structure of **8a** has been determined by X-ray crystallography (see Figure 5). The complex adopts an octahedral coordination geometry in which the two PEt_3 ligands assume *trans*-diaxial positions,

(41) Muetterties, E. L., Ed. *Transition Metal Hydrides*; Marcel Dekker: New York, 1971, and references cited therein.

(42) Small quantities of *mer*-CH=C(Me)CH=C(Me)CH_2Ir(PEt_3)$_3$(H) (**1b**) are observed in the reaction solution by NMR. This product is apparently generated by trapping of intermediate **J** (Scheme 10) with PEt_3. However, **1b** also reacts slowly with excess H_2 to produce iridium polyhydrides.

Scheme 9

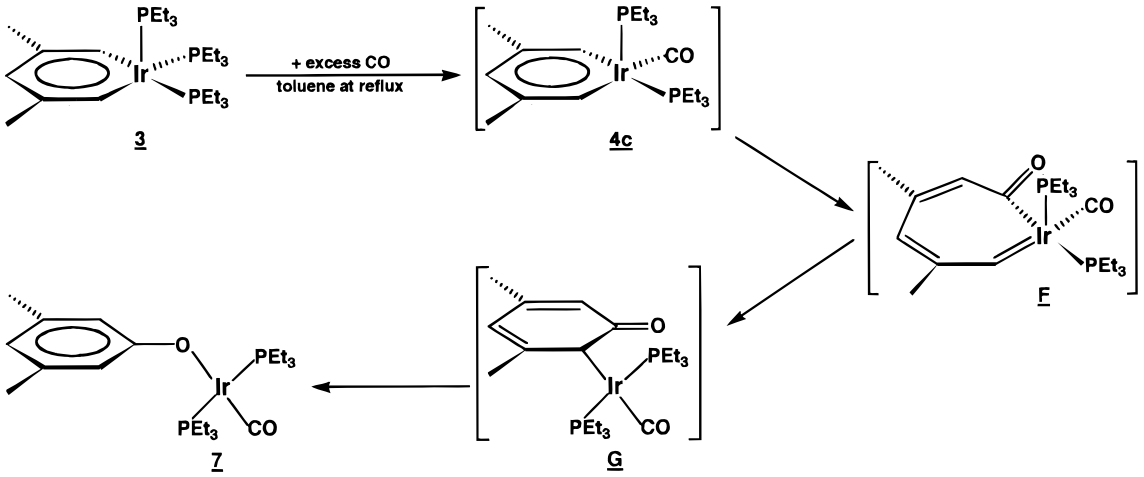

Scheme 10

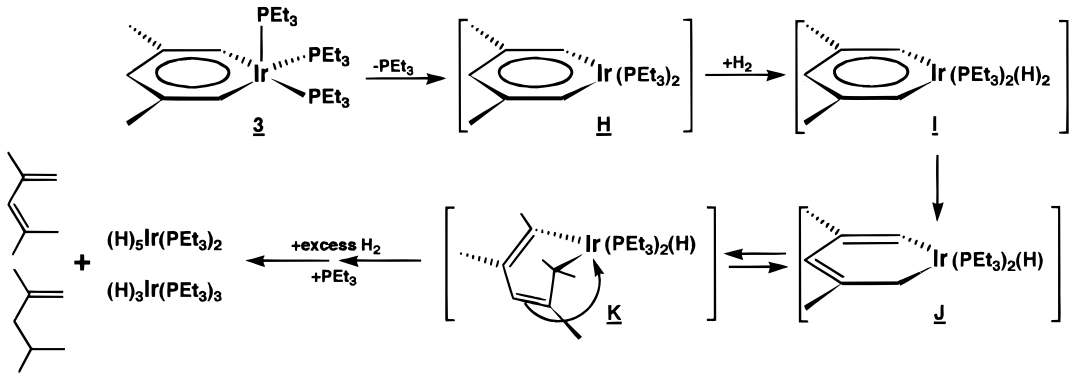

Scheme 11

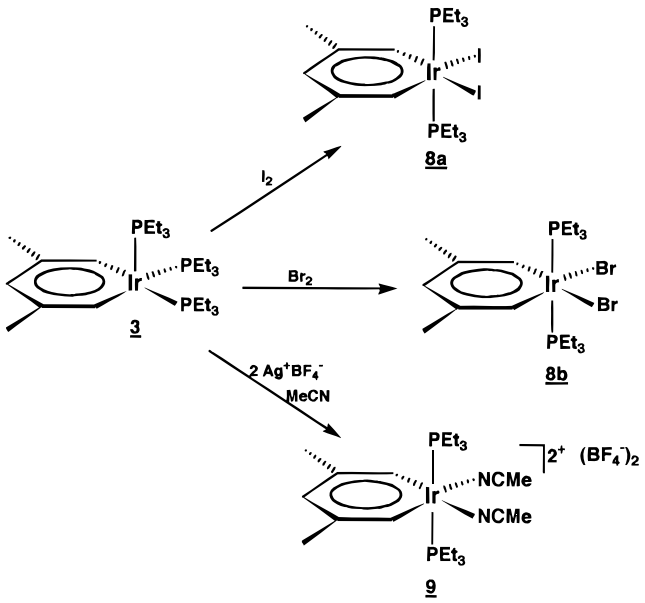

while the two iodide ligands reside *trans* to C1 and C5 of the metallacycle. The aromatic ring is nearly planar, with the iridium atom lying just 0.13 Å out of the ring carbon plane (C1/C2/C3/C4/C5). The dihedral angle between the ring carbon plane and C1/Ir1/C5 is a mere 5.3°. The ring C−C bond distances range from 1.36(4) to 1.42(4) Å and average 1.39 Å, while the Ir−C bond distances range from 1.92(2) to 1.99(2) Å and average 1.95 Å.

The ^{1}H NMR signals for ring protons H1/H5 and H3 in **8a** are shifted even more dramatically downfield than those in **3**, appearing at δ 13.95 and 7.86, respectively, in acetone-d_6. In addition to the ring current and neighboring group anisotropic effects described earlier, these shifts probably reflect the inductive effect of an oxidized iridium center and two electronegative iodine atoms in the ring plane.[43] The ^{13}C{^{1}H} NMR spectrum of **8a** follows the same chemical shift pattern with C1/C5, C3, and C2/C4 appearing at δ 215.1, 161.6, and 134.8, respectively. As expected, the H1/H5 and C1/C5 signals show essentially no coupling to the *trans*-diaxial phosphine ligands.

As shown in Scheme 11, treatment of iridabenzene **3** with bromine (Br_2) produces the dark blue oxidative addition product $\overline{CH{=}C(Me)CH{=}C(Me)CH{=}Ir}(PEt_3)_2(Br)_2$ (**8b**). The NMR spectra of **8b** are closely analogous to those of **8a**, strongly suggesting that the two compounds are isostructural. Iridabenzene **3** can also be oxidized with conventional oxidizing agents such as Ag^+. For example, treatment of **3** with 2 equiv of $Ag^+BF_4^-$ in acetonitrile leads to the clean production of $\overline{CH{=}C(Me)CH{=}C(Me)CH{=}Ir}(PEt_3)_2(NCMe)_2]^{2+}(BF_4^-)_2$ (**9**). The ^{1}H NMR chemical shifts for H1/H5 and H3 in **9** are δ 13.02 and 8.16, respectively, while ^{13}C chemical shifts for C1/C5, C3, and C2/C4 are δ 210.8, 172.3, and 138.3, respectively. The H1/H5 and C1/C5 signals show essentially no phosphorus coupling, indicating that the phosphines occupy *trans*-diaxial positions in the metal's octahedral coordination sphere.[44]

3. Cycloadditions. Iridabenzene **3** is ideally suited to participate in cycloaddition reactions because (a) it

(43) Becker, E. D. *High Resolution NMR*, 2nd ed.; Academic Press: New York, 1980; pp 55−84.

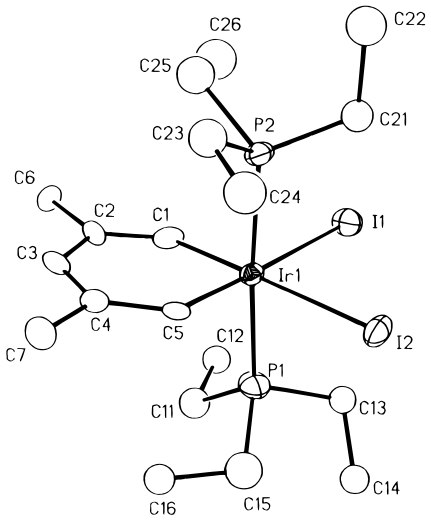

Figure 5. ORTEP drawing of CH=C(Me)CH=C(Me)-CH=Ir(PEt$_3$)$_2$(I)$_2$ (**8a**). Compound **8a** crystallized with two independent molecules in the unit cell; molecule **1** is reported here. Selected bond distances (Å) with estimated standard deviations: Ir1−I1, 2.822(3); Ir1−I2, 2.818(2); Ir1−P1, 2.371(8); Ir1−P2, 2.370(7); Ir1−C1, 1.988(24); Ir1−C5, 1.963(23); C1−C2, 1.378(37); C2−C3, 1.390(35); C2−C6, 1.576(36); C3−C4, 1.420(39); C4−C5, 1.390(34); C4−C7, 1.549(37). Selected bond angles (deg) with estimated standard deviations: C1−Ir1−C5, 89.0(10); Ir1−C1−C2, 127.9(19); C1−C2−C3, 125.3(24); C1−C2−C6, 114.5(21); C3−C2−C6, 119.9(22); C2−C3−C4, 124.3(23); C3−C4−C5, 122.1(23); C3−C4−C7, 118.1(22); C5−C4−C7, 119.8(23); Ir1−C5−C4, 130.7(18).

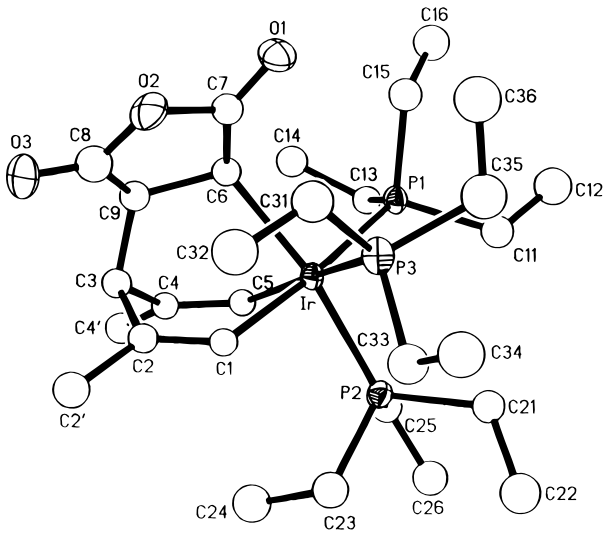

Figure 6. ORTEP drawing of CH=C(Me)CHC(Me)=CHIr-[CHC(O)OC(O)CH](PEt$_3$)$_3$ (**12**). Selected bond distances (Å) with estimated standard deviations: Ir−P1, 2.404(2); Ir−P2, 2.332(2); Ir−P3, 2.407(2); Ir−C1, 2.083(7); Ir−C5, 2.089(7); Ir−C6, 2.243(7); C1−C2, 1.317(10); C2−C2′, 1.489(11); C2−C3, 1.531(11); C3−C4, 1.537(9); C3−C9, 1.539(11); C4−C4′, 1.484(10); C4-C5, 1.339(10); C6-C9, 1.509(11). Selected bond angles (deg) with estimated standard deviations: P1−Ir−P2, 94.3(1); P1−Ir−P3, 101.2-(1); P2−Ir−P3, 95.5(1); P1−Ir−C1, 174.1(2); P2−Ir−C6, 165.0(2); P3−Ir−C5, 167.9(2); C1−Ir−C5, 85.1(3); C1−Ir−C6, 87.3(3); C5−Ir−C6, 79.4(3); Ir−C1−C2, 123.6(5); C1−C2−C2′, 124.3(7); C1−C2−C3, 119.1(7); C2′−C2−C3, 116.6-(7); C2−C3−C4, 109.9(6); C2−C3−C9, 110.1(6); C4−C3−C9, 107.6(6); C3−C4−C4′, 119.0(6); C3−C4−C5, 117.7(6); C4′−C4−C5, 123.3(6); Ir−C5−C4, 123.7(5).

has a square-pyramidal coordination geometry with an open face that allows close approach by substrate molecules and (b) it possesses a reactive metalladiene moiety held rigidly in a cisoid geometry. Hence, **3** reacts with a wide variety of cycloaddition substrates, including olefins, heteroolefins, and heterocumulenes. While some of these reactions may proceed via stepwise mechanisms,[45] the majority are thought to occur in a concerted fashion.[46] For concerted cycloadditions, the key orbital interaction would involve the "effective HOMO" of the electron-rich iridabenzene,[47] pictured in Figure 3, and the LUMO of the substrate molecule, which is usually a π^* orbital. Recall that the effective HOMO of **3** is derived from a strong bonding interaction between a hybrid metal d orbital (d_{xz}/d_{z^2}) and the 3π orbital of the organic ring fragment.[32] As a result, the wave function has the same phase on Ir and C1/C5 but the opposite phase on C3.

As shown in Scheme 12, treatment of compound **3** with molecular oxygen, nitrosobenzene, maleic anhydride, or carbon disulfide leads to clean 4 + 2 cycloaddition reactions[48] in which the substrate adds across iridium and C3 of the iridabenzene ring, producing compounds **10**−**13**, respectively. Similarly, **3** undergoes a cheleotropic 4 + 2 cycloaddition[48] with sulfur dioxide to produce adduct **14**. These reactions are all accompanied by a dramatic color change from red (iridabenzene) to light yellow (adducts) and generate the products in high yield.

Compounds **10**, **12**, and **14** have been fully characterized by X-ray crystallography.[49] ORTEP drawings of **12** and **14**, along with selected bond distances and angles, are presented in Figures 6 and 7, respectively. The structure of **10** has been described in a previous communication.[1e] In each structure, the cycloaddition substrate has added across the open face of square-pyramidal **3**, generating an octahedral adduct. The resulting iridacyclohexadiene ring is boat-shaped, with Ir and C3 lying significantly out of the C1/C2/C4/C5 plane. In **12**, for example, Ir and C3 lie 0.771 and 0.656 Å, respectively, from the C1/C2/C4/C5 plane. The dihedral angles made by planes C1/Ir/C5 and C2/C3/C4 with the C1/C2/C4/C5 plane are 30.1 and 48.1°, respectively. In **14**, the bending of the ends of the boat is even more severe, due to the demands of the five-membered rings. Ir and C3 lie 0.994 and 0.701 Å from the C1/C2/C2a/C1a plane, while the dihedral angles made by C1/Ir/C1a and C2/C3/C2a with C1/C2/C2a/C1a

(44) Compounds **8a,b** and **9** are probably best viewed as Ir(III) species in which the carbon fragment of the iridabenzene ring (C_5H_3-Me_2) serves as a monoanionic ligand. The Ir−C π interaction results from back-bonding of metal d_{xz} electrons into the empty 3π orbital of the carbon fragment.

(45) For example, the reaction with triplet oxygen almost certainly involves a stepwise radical pathway.

(46) Unfortunately, we have not been able to find *cis*- and *trans*-EHC=CHE substrates that react cleanly with **3** and would allow the stereochemistry of the addition to be probed.

(47) We use the term "effective HOMO" because there are actually three filled, essentially nonbonding d orbitals ($d_{x^2-y^2}$, d_{yz}, and d_{xz}/d_{z^2} hybrid) that lie slightly higher in energy than the orbital of interest. However, these d orbitals do not appear to participate in the cycloaddition reactions.

(48) For a good summary of cycloaddition reactions involving organic components, see: Lowry, T. H.; Richardson, K. S. *Mechanisms and Theory in Organic Chemistry*; Harper and Row: New York, 1976; pp 626−645, and references cited therein.

(49) X-ray analysis of a CO derivative of **11** (in which one PEt$_3$ ligand is replaced by CO) has confirmed the proposed structure.

Scheme 12

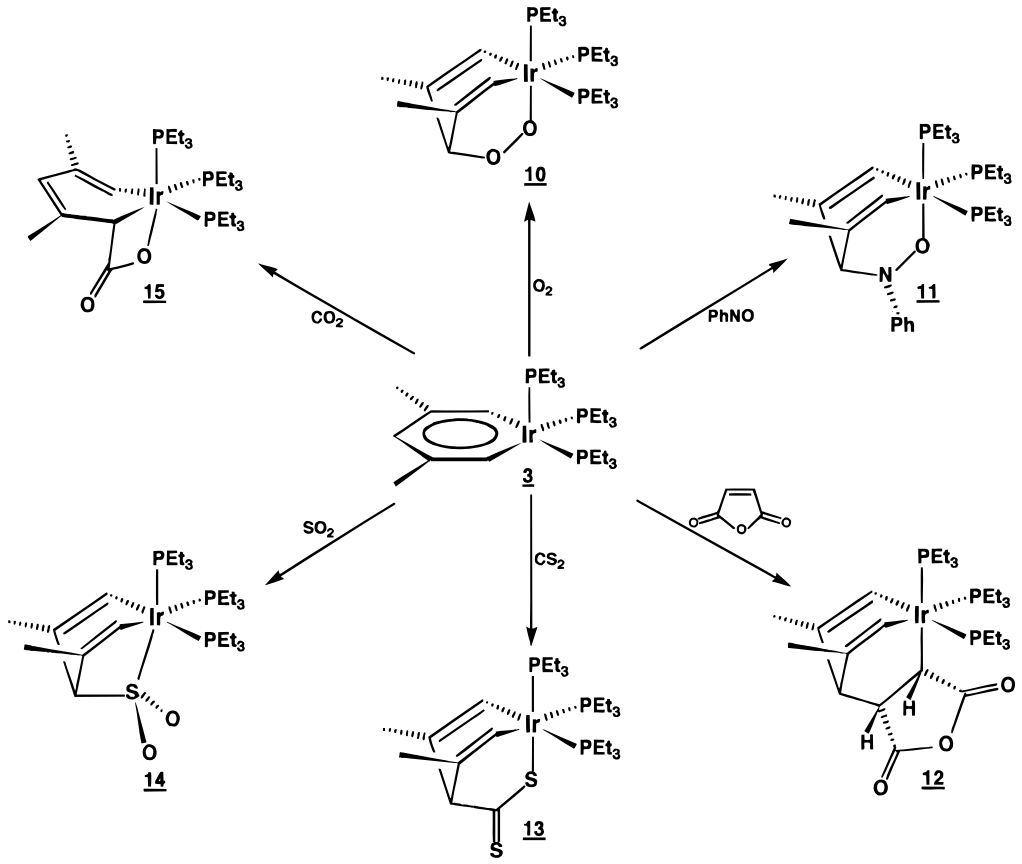

are 40.0 and 55.8°, respectively. Bonding within the 1-iridacyclohexa-2,5-diene rings is localized, as expected.

Unlike iridabenzene **3**, adducts **10**−**14** are stereochemically rigid by NMR. Compounds **10**, **11**, **13**, and **14** possess mirror plane symmetry;[50] therefore, the $^{31}P\{^{1}H\}$ NMR spectra of these species consist of a doublet (two equivalent phosphines *trans* to the ring) and a triplet (unique phosphine *trans* to substrate). Adduct **12** possesses no symmetry, so that all three phosphines exhibit separate doublet-of-doublet resonances in the $^{31}P\{^{1}H\}$ NMR.

In the ^{13}C NMR spectra of adducts **10**−**14**, the C1/C5 signals shift upfield to δ 122−136 from their position of δ 167.3 in **3**, reflecting the loss of carbenic character. These signals are split by phosphorus coupling into doublet-of-triplet patterns with the large doublet coupling due to the *trans* PEt_3 ligand and the small triplet coupling due to the *cis* PEt_3's. The C3 signal in **10**−**14** shifts upfield to δ 58−101 from its position of δ 129.8 in **3**, reflecting the sp^3 hybridization of C3 in the adducts. Similarly, the H1/H5 signals in **10**−**14** shift upfield to δ 6.75−7.40 from their position of δ 10.91 in **3**, while the H3 signal moves upfield to δ 3.25−4.75 from δ 7.18 in **3**.

Unlike the cycloaddition reactions described above, iridabenzene **3** reacts with CO_2 to produce a 2 + 2 cycloaddition product (**15**, Scheme 12).[51] If this reaction is concerted, it must proceed via a perpendicular approach of the CO_2 molecule to the Ir−C_α bond, as required for a 2s + 2a cycloaddition.[48] The minimal steric demands of CO_2 and the presence of a second set of π orbitals may provide stabilization for this perpendicular orientation. Alternatively, this reaction may proceed stepwise by nucleophilic attack of an iridabenzene α ring carbon on the electrophilic carbon of CO_2, followed by iridium−oxygen bond formation. Other electrophilic reagents, including H^+ and BF_3, have been shown to react at the iridabenzene α ring carbon (*vide infra*), a site with substantial basic character.

The X-ray crystal structure of **15**, which we reported earlier,[1j] shows the iridacyclohexadiene ring in a half-boat conformation with Ir lying 0.649 Å out of the C1/C2/C3/C4/C5 plane. The dihedral angle between plane C1/Ir/C5 and plane C1/C2/C3/C4/C5 is 24.4°. Bonding within the 1-iridacyclohexa-2,4-diene ring is localized, as expected. The $^{31}P\{^{1}H\}$ NMR spectrum of **15** consists of three separate doublet-of-doublet signals due to the three inequivalent PEt_3 ligands. The chemical shifts for C1 and H1 are similar to those seen in adducts **10**−**14**, but C3 and H3 are much more downfield (δ 126.0 and δ 5.5, respectively) because C3 retains its sp^2 hybridization in **15**. C5 and H5 shift far upfield (to δ 23.7 and δ 3.2, respectively), reflecting C5's sp^3 hybridization. Both C1 and C5 exhibit the characteristic doublet-of-triplet splitting pattern that results from phosphorus coupling.

Finally, treatment of **3** with nitrous oxide leads to ring contraction and formation of iridacyclopentadiene complex **16** (Scheme 13).[52] The same product is obtained when **3** is reacted with amine *N*-oxides, including 4-methylmorpholine *N*-oxide and trimethylamine *N*-oxide. One reasonable pathway for this reaction involves initial formation of metallaepoxide **L** (Scheme

(50) In the case of **11**, mirror-plane symmetry is apparently maintained by rapid inversion about the nitrogen center.

(51) For a related reaction, see: Klein, D. P.; Bergman, R. G. *J. Am. Chem. Soc.* **1989**, *111*, 3079.

(52) X-ray analysis of a triflate derivative of **16** (in which $O_3SCF_3^-$ has replaced H^-) has confirmed the proposed structure.

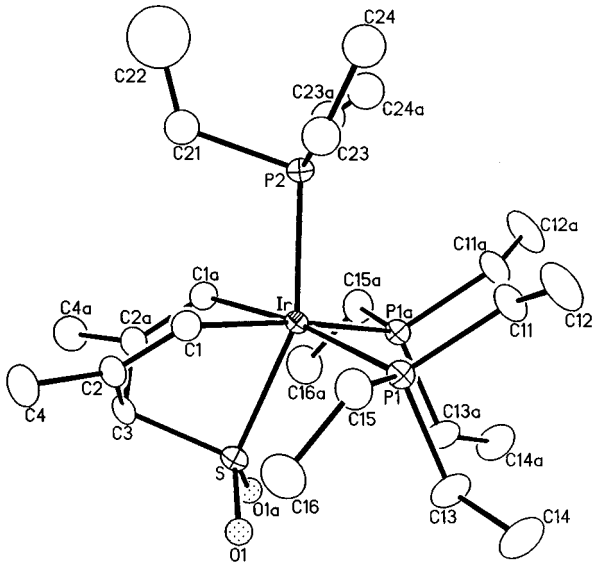

Figure 7. ORTEP drawing of $\overline{CH{=}C(Me)CHC(Me){=}CH}Ir[S(O)_2](PEt_3)_3$ (**14**). Selected bond distances (Å) with estimated standard deviation: Ir−P1, 2.399(2); Ir−P2, 2.338(4); Ir−C1, 2.094(8); Ir−S, 2.347(3); C1−C2, 1.323(12); C2−C3, 1.500(11); C2−C4, 1.475(15); C3−S, 1.844(13); S−O1, 1.471(7). Selected bond angles (deg) with estimated standard deviations: S−Ir−P1, 95.3(1); S−Ir−P2, 157.3(1); P1−Ir−P2, 99.9(1); S−Ir−C1, 77.1(2); P1−Ir−C1, 89.5(2); P2−Ir−C1, 86.2(2); P1−Ir−P1a, 95.4(1); P1−Ir−C1a, 171.3(2); C1−Ir−C1a, 84.8(5); Ir−S−O1, 117.8(3); Ir−S−C3, 90.1(4); O1−S−C3, 108.5(3); O1−S−O1a, 111.2(5); Ir−C1−C2, 118.3(6); C1−C2−C3, 114.8(8); C1−C2−C4, 125.5(9); C3−C2−C4, 119.7(9); S−C3−C2, 102.9(6); C2−C3−C2a, 111.4(10).

Scheme 13

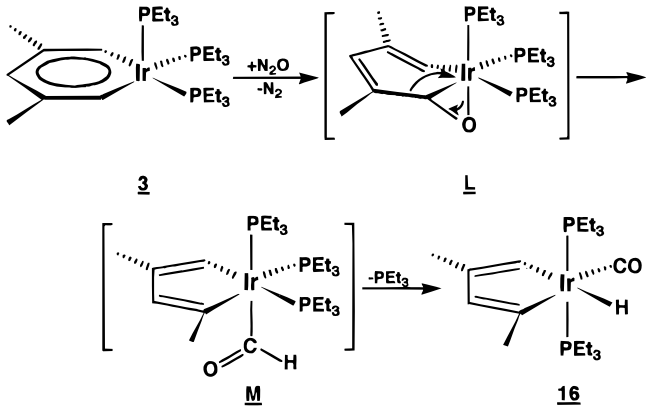

13). Rearrangement would lead to formyl species **M**, and migration of the formyl hydrogen ("retroinsertion") would then generate the carbonyl-hydride product **16**. Alternatively, rearrangement of the metallaepoxide (**L**) could generate a metallacyclohexadienone hydride, which could retroinsert to produce **16**.

The NMR spectra for **16** are, of course, significantly different from those of adducts **10**−**15**. The *trans*-diaxial phosphines are equivalent and appear as a singlet in the $^{31}P\{^1H\}$ NMR spectrum. All four ring carbon atoms appear in the downfield region of the ^{13}C NMR spectrum (δ 135−151), as expected for sp^2 carbons, while the carbonyl carbon resonates at δ 177.9. Ring carbons C1 and C4, as well as the carbonyl carbon, are split into closely spaced triplets by weak coupling to the equivalent PEt_3 ligands. Ring hydrogens H1 and H3 resonate at δ 7.3 and δ 6.4, respectively, in the ^1H NMR spectrum, while the metal hydride appears as a phosphorus-coupled triplet at δ −10.6.

4. Electrophilic Addition. Iridabenzene **3** reacts with electrophiles at the electron-rich α ring carbon atoms, C1/C5. Hence, treatment of **3** with 1 equiv of $H^+O_3SCF_3^-$ results in clean protonation at C_α and production of $[\overline{CH{=}C(Me)CH{=}C(Me)CH_2}Ir(PEt_3)_3]^+O_3SCF_3^-$ (**2**)[1a] (see Scheme 14). Similarly, treatment of **3** with acetylacetone ($pK_a \approx 9$) or with diethyl malonate ($pK_a \approx 13$) leads to protonation at C_α. However, in these cases, the cationic pentadienediyl product is rapidly attacked by the acid anion, generating neutral bis-PEt_3 compounds **17** and **18**, respectively (Scheme 13). Iridabenzene **3** does not react with acids having pK_a's above ~15, including water.[53]

Compounds **17** and **18** are readily characterized by NMR. In each case, the $^{31}P\{^1H\}$ spectrum consists of a single sharp peak. In the ^{13}C NMR, ring carbons C1, C2, C3, and C4 appear downfield in the typical region for sp^2-hybridized centers (δ 118−135), while C5 appears far upfield (δ ~−10). The C1 and C5 signals are split into closely spaced triplets as a result of weak phosphorus coupling. In the ^1H NMR, H1 and H3 resonate downfield (δ ~7.7 and 5.8, respectively) and appear as sharp singlets, while H5 resonates at δ ~3.5 and is split into a triplet by the equivalent *trans*-diaxial phosphines.

When iridabenzene is treated with 2 equiv of a strong acid such as $H^+O_3SCF_3^-$, protonation occurs at *both* C1 and C5, generating $[(\eta^5\text{-}2,4\text{-dimethylpentadienyl})Ir(PEt_3)_3]^{2+}(O_3SCF_3^-)_2$ (**19**, Scheme 14). In solution, compound **19** exhibits mirror-plane symmetry. Hence, the $^{31}P\{^1H\}$ NMR spectrum consists of a doublet (due to two equivalent phosphines located under the pentadienyl chain) and a triplet (due to the unique phosphine situated under the open pentadienyl mouth). These signals do not broaden significantly upon heating to 60 °C, indicating that the η^5-pentadienyl ligand does not rotate with respect to the $Ir(PEt_3)_3$ framework on the NMR time scale. In the ^{13}C NMR, pentadienyl carbons C1/C5, C3, and C2/C4 resonate at δ 50.1, 94.6, and 142.7, respectively, while in the ^1H NMR, $H1_{inner}$, $H1_{outer}$, and H3 resonate at δ 2.41, 3.83, and 7.29, respectively.

Finally, treatment of iridabenzene **3** with excess boron trifluoride leads to the formation of a novel (η^6-borabenzene)metal complex,[54] $[(\eta^6\text{-}1\text{-fluoro-}3,5\text{-dimethyl-}1\text{-borabenzene})Ir(PEt_3)_3]^{2+}(BF_4^-)_2$ (**20**, Scheme 14). Although the detailed mechanism of this reaction is not known, one reasonable pathway, shown in Scheme 15, involves initial electrophilic attack of BF_3 at ring carbon C5, generating intermediate **N**. Migration of ring carbon C1 to boron with concomitant removal of fluoride as BF_4^- closes the boracyclohexadienyl ring, generating **O**. Finally, reaction of **O** with a third equivalent of BF_3 results in removal of another fluoride as BF_4^- and aromatization of the borabenzene ring.

The structure of **20**, as determined by single-crystal X-ray diffraction, is shown in Figure 8. The boraben-

(53) House, H. O. *Modern Synthetic Reactions*, 2nd ed.; W. A. Benjamin: Menlo Park, CA, 1972; p 494.

(54) For a good summary of (borabenzene)metal chemistry, see: Herberich, G. E.; Ohst, H. In *Advances in Organometallic Chemistry*; Stone, F. G. A., West, R., Eds.; Academic Press: Orlando, FL, 1986; Vol. 25, pp 199−236.

Scheme 14

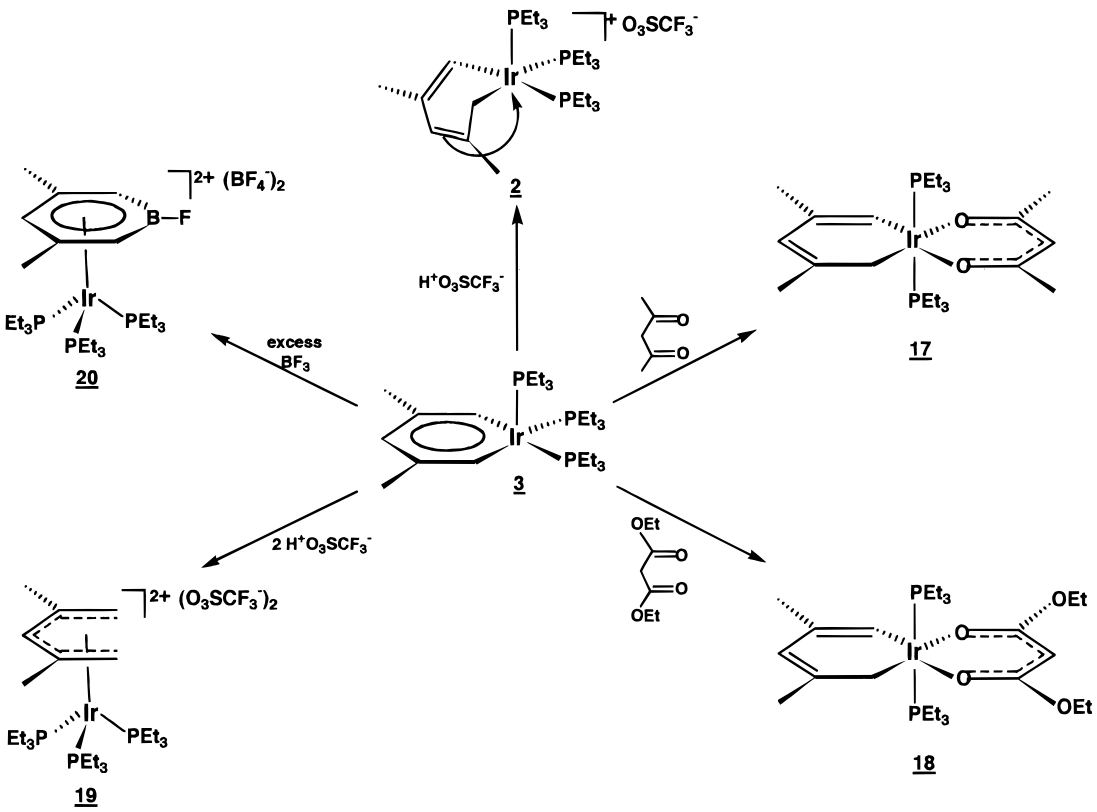

Scheme 15

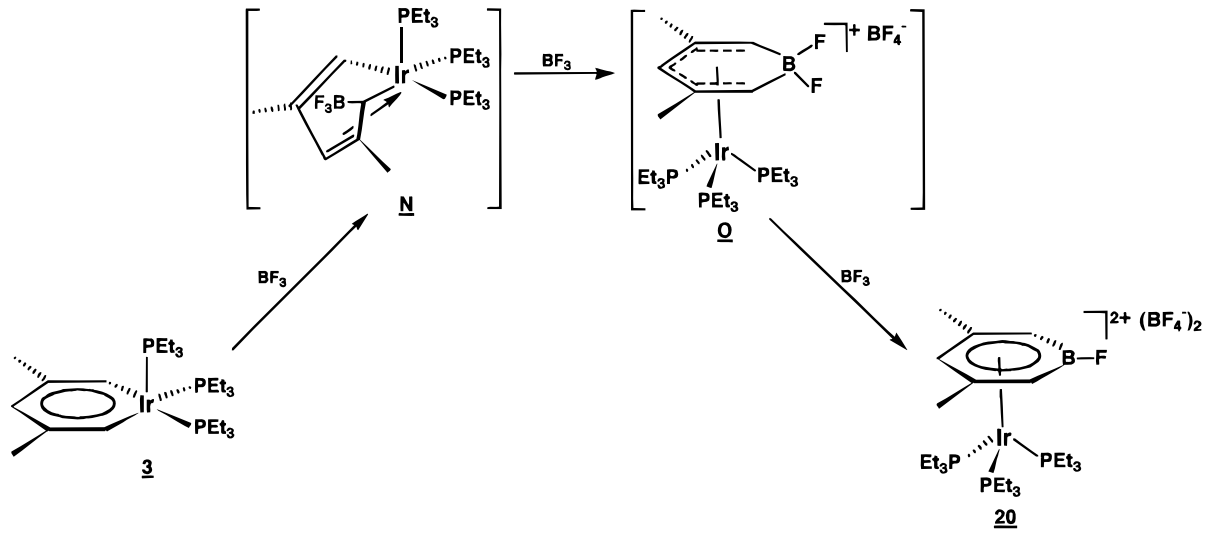

zene ring exhibits a chairlike distortion from planarity, with B1 lying 0.229 Å above the C1/C2/C4/C5 plane (away from the iridium center) and C3 lying 0.153 below the same plane (toward Ir). The dihedral angles made by planes C1/B1/C5 and C2/C3/C4 with the C1/C2/C4/C5 plane are 15.9 and 12.8°, respectively. Among the six iridium-ring atom bonds, the Ir−C3 interaction is the shortest (2.267 Å) and the Ir−B bond is the longest (2.534 Å). Distances and angles within the ring are typical for metal-coordinated borabenzene; of particular note are the relatively long B−C distances (1.536(14) and 1.514(10) Å) and the contracted C−B−C angle (113.8(7)°).

In acetone solution at room temperature, the η^6-borabenzene ligand rotates with respect to the $Ir(PEt_3)_3$ moiety. Hence, the $^{31}P\{^1H\}$ NMR spectrum of **20** at 25 °C consists of a single resonance. However, as the sample is cooled, borabenzene rotation is slowed down and decoalescence of the ^{31}P NMR signal occurs. At −90 °C, the stopped-exchange limiting spectrum—a doublet (intensity 2) and a triplet (intensity 1)—is observed. Line shape analysis of the ^{31}P NMR spectrum allows us to calculate a free energy of activation ($\Delta G^{\ddagger}$) of 11.3 ± 0.2 kcal/mol. In the $^{13}C\{^1H\}$ NMR, borabenzene carbons C1/C5, C3, and C2/C4 resonate at δ 78.3, 79.3, and 152.1, respectively, while in the ^1H NMR, H1/H5 and H3 resonate at δ 4.70 and 6.33, respectively.

5. Coordination of $Mo(CO)_3$. Iridabenzene **3** cleanly displaces *p*-xylene from (*p*-xylene)$Mo(CO)_3$ in tetrahydrofuran solvent, producing the metal-coordinated metallabenzene complex [η^6-CH=C(Me)CH=C(Me)CH=Ir-$(PEt_3)_3$]$Mo(CO)_3$ (**21**) (see Scheme 16).[1e,f] The X-ray crystal structure of **21**, reported earlier,[1e,f] shows that

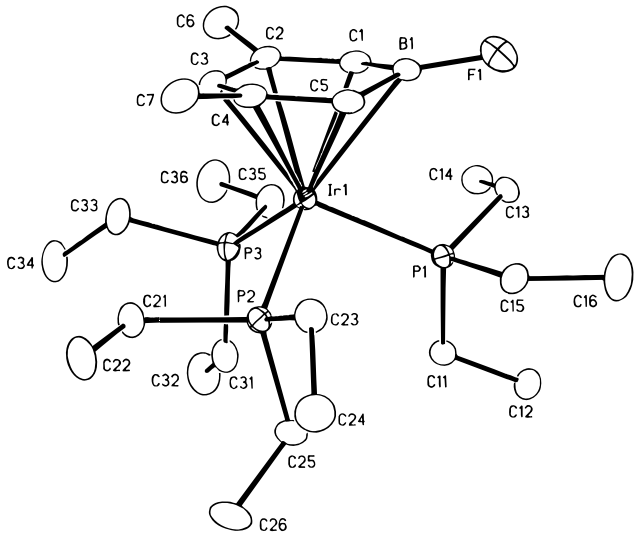

Figure 8. ORTEP drawing of [(η^6-1-fluoro-3,5-dimethyl-1-borabenzene)Ir(PEt_3)$_3$]$^{2+}$(BF_4^-)$_2$ (**20**). Selected bond distances (Å) with estimated standard deviations: Ir1−P1, 2.375(2); Ir1−P2, 2.343(2); Ir1−P3, 2.368(2); Ir1−B1, 2.534-(8); Ir1−C1, 2.351(7); Ir1−C2, 2.384(9); Ir1−C3, 2.267(9); Ir1−C4, 2.409(8); Ir1−C5, 2.354(8); B1−F1, 1.377(10); B1−C1, 1.536(14); B1−C5, 1.514(10); C1−C2, 1.390(12); C2−C3, 1.431(10); C2−C6, 1.518(15); C3−C4, 1.430(13); C4−C5, 1.403(12); C4−C7, 1.502(11). Selected bond angles (deg) with estimated standard deviations: P1−Ir1−P2, 95.7(1); P1−Ir1−P3, 99.2(1); P2−Ir1−P3, 93.3(1); P1−Ir1−C3, 152.4(2); P2−Ir1−C1, 159.7(2); P3−Ir1−C5, 158.7(2); B1−C1−C2, 119.8(7); C1−C2−C3, 120.0(8); C1−C2−C6, 121.5-(7); C6−C2−C3, 118.5(8); C2−C3−C4, 122.3(7); C3−C4−C7, 117.0(8); C3−C4−C5, 118.1(7); C7−C4−C5, 124.8(8); C4−C5−B1, 121.6(8); C5−B1−C1, 113.8(7); C5−B1−F1, 124.1(8); F1−B1−C1, 122.0(7).

Scheme 16

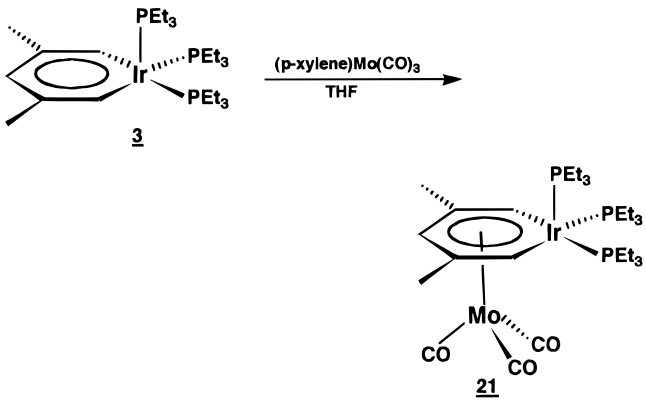

the bonding within the metallabenzene ring is still fully delocalized, but the average C−C and Ir−C bond distances (1.41 and 2.03 Å, respectively) are slightly longer than those in parent **3** (C−C_{av} = 1.38 Å, Ir−C_{av} = 2.00 Å). The iridium atom in **21** resides 0.30 Å out of the plane of the five ring carbons (C1/C2/C3/C4/C5), and the dihedral angle between this plane and the plane C1/Ir/C5 is 11.7°. The molybdenum atom is strongly π-complexed to all six atoms of the arene ring. The Mo−Ir distance is 2.978(1) Å, while the Mo−C_{ring} distances range from 2.318(10) to 2.404(9) Å; the shortest bond is with C3.

Unlike **3**, which undergoes a very low energy intramolecular phosphine exchange process in solution (*vide supra*), **21** is stereochemically rigid, even upon heating to 60 °C. Hence, the $^{31}P\{^1H\}$ spectrum of **21** consists of a doublet (equivalent basal phosphines) and a triplet (axial phosphine). The ^1H NMR signals for the ring protons in **21** shift upfield from their positions in **3**, as is normally observed when arenes coordinate to metal fragments. Proton H1/H5 in **21** appears at δ 8.08 (vs 10.91 in **3**), while H3 resonates at δ 6.25 (vs 7.18 in **3**). The ring carbons show a similar upfield ^{13}C NMR shift. Hence, C1/C5, C2/C4, and C3 resonate at δ 135.7, 107.9, and 99.5 in **21** vs δ 167.6, 132.0, and 129.9 in **3**. The H1/H5 signal is a doublet (J = 20.7 Hz) due to strong coupling to the *cis* basal phosphine.

The metallabenzene moiety in **21** rotates freely with respect to the $Mo(CO)_3$ fragment.[55] As a result, the carbonyl carbon atoms in **21** give rise to a sharp singlet in the $^{13}C\{^1H\}$ NMR spectrum, even at −80 °C. The infrared spectrum of **21** shows the presence of two intense ν(CO) bands (A_1 and E), as is characteristic of (η^6-arene)$Mo(CO)_3$ complexes. The very low energy of these bands (1918 and 1836 cm^{-1}) indicates substantial π-back-bonding and reflects the extremely electron-rich nature of arene **3**. By comparison, the ν(CO) bands for (η^6-*p*-xylene)$Mo(CO)_3$ appear at 1975 and 1901 cm^{-1}.[56] Since the stability of (η^6-arene)$Mo(CO)_3$ complexes increases with increasing arene basicity, it is not surprising that **3** cleanly displaces organic arenes from (η^6-arene)$Mo(CO)_3$ complexes in THF solvent.[57]

Summary

In this paper, we have reported the first thorough investigation of the physical and chemical properties of a metallabenzene complex, CH=C(Me)CH=C(Me)CH=Ir-(PEt_3)$_3$ (**3**). The X-ray crystal structure of "iridabenzene" **3** and its solution-phase NMR spectra are consistent with the presence of an aromatic ring system. In particular, bonding within the planar metallacycle is fully delocalized, and ring proton signals are shifted far downfield in the ^1H NMR spectrum. The key orbital interaction which gives rise to the stable, aromatic character of **3** involves a metal d orbital (d_{xz}/d_{z^2} hybrid) and the 3π orbital of the organic moiety.

Compound **3** undergoes a variety of reactions, including ligand exchange, oxidation, cycloaddition, electrophilic addition, and arene exchange. The ligand exchange and oxidation reactions lead to products in which the aromatic ring system is retained. In contrast, the cycloaddition reactions disrupt the aromaticity of **3**, generating octahedral Ir(III) products in which the iridabenzene ring has been converted to a boat-shaped 1-iridacyclohexa-2,5-diene ring (4 + 2 cycloaddition) or a half-boat 1-iridacyclohexa-2,4-diene ring (2 + 2 cycloaddition). Electrophiles add to compound **3** at the electron-rich α ring carbons, producing a variety of interesting products, including (η^5-pentadienyl)Ir and (η^6-borabenzene)Ir species. Finally, compound **3** participates in arene exchange reactions; hence, treatment of (*p*-xylene)$Mo(CO)_3$ with iridabenzene **3** results in clean *p*-xylene displacement and production of (η^6-iridabenzene)$Mo(CO)_3$.

We are currently investigating other metallacycles that possess the same favorable electronic interactions

(55) In most (η^6-arene)$Mo(CO)_3$ complexes, arene ring rotation occurs with only a small activation barrier. See: Mann, B. E. In *Comprehensive Organometallic Chemistry*; Wilkinson, G., Stone, F. G. A., Abel, E. W., Eds.; Pergamon: Oxford, U.K., 1982; Vol. 3, pp 89−113.

(56) Barbeau, C.; Turcotte, J. *Can. J. Chem.* **1976**, *54*, 1612.

(57) Muetterties, E. L.; Bleeke, J. R.; Sievert, A. C. *J. Organomet. Chem.* **1979**, *178*, 197.

as **3** and might, therefore, exhibit aromatic properties. Results of these efforts will be described in future papers.

Experimental Section

General Comments. All manipulations were carried out under a nitrogen atmosphere, using either glovebox or double-manifold Schlenk techniques. Solvents were stored under nitrogen after being distilled from the appropriate drying agents. Deuterated NMR solvents were obtained from Cambridge Isotope Laboratories in 1 g sealed vials and used as received. The following reagents were used as obtained from the supplier indicated: lithium diisopropylamide (Aldrich), trimethylphosphine (Strem), trimethyl phosphite (Strem), carbon monoxide (Air Products), hydrogen (Air Products), iodine (Fisher), bromine (Fisher), silver tetrafluoroborate (Aldrich), nitrosobenzene (Aldrich), maleic anhydride (Aldrich), carbon disulfide (Aldrich), sulfur dioxide (Aldrich), carbon dioxide (Matheson), nitrous oxide (Aldrich), 2,4-pentanedione (Aldrich), diethyl malonate (Aldrich), trifluoromethanesulfonic acid (Aldrich), and boron trifluoride (Matheson).

Detailed syntheses and full NMR characterization of compounds **1** and **2** are given in ref 1c. In compound **2**, J_{H-P} for H1 was incorrectly reported as 22 Hz; the correct value is 11 Hz. Synthesis and NMR data for compound **21** are reported in ref 1f.

NMR experiments were performed on a Varian Unity-300 spectrometer (^{1}H, 300 MHz; ^{13}C, 75 MHz; ^{31}P, 121 MHz), a Varian Unity-500 spectrometer (^{1}H, 500 MHz; ^{13}C, 125 MHz; ^{31}P, 202 MHz), or a Varian VXR-600 spectrometer (^{1}H, 600 MHz; ^{13}C, 150 MHz; ^{31}P, 242 MHz). ^{1}H and ^{13}C spectra were referenced to tetramethylsilane, while ^{31}P spectra were referenced to external H_3PO_4. In general, ^{1}H connectivities were determined from COSY (^{1}H−^{1}H correlation spectroscopy) data. APT (attached proton test), HETCOR (^{13}C−^{1}H heteronuclear correlation spectroscopy), and HMQC (^{1}H-detected multiple quantum coherence) experiments aided in assigning some of the ^{1}H and ^{13}C peaks.

The infrared spectra were recorded on a Perkin-Elmer 283B or Mattson Polaris FT IR spectrometer.

Microanalyses were performed by Galbraith Laboratories, Inc., Knoxville, TN.

Synthesis of $\overline{CH{=}C(Me)CH{=}C(Me)CH{=}}Ir(PEt_3)_3$ (3). Compound **2**, $[\overline{CH{=}C(Me)CH{=}C(Me)CH_2}Ir(PEt_3)_3]^+O_3SCF_3^-$ (0.50 g, 6.3×10^{-4} mol), was mixed with lithium diisopropylamide (0.068 g, 6.3×10^{-4} mol) and dissolved in 10 mL of cold (−30 °C) acetone. The resulting solution was shaken by hand for 10 min and then stored at −30 °C for 1 h. After removal of the solvent under vacuum, the red residue was extracted with pentane and filtered. The pentane solvent was then removed under vacuum, and the residue was redissolved in a minimal quantity of acetone and cooled to −30 °C. Red crystals of **3** were obtained overnight. Yield: 0.30 g, 75%. Anal. Calcd for $C_{25}H_{54}IrP_3$: C, 46.92; H, 8.52. Found: C, 46.57, H, 8.60.

^{1}H NMR (acetone-d_6, 22 °C): δ 10.91 (quartet, J_{H-P} = 7.2 Hz, 2, H1/H5), 7.18 (br s, 1, H3), 2.49 (s, 6, ring CH_3's), 1.85−1.74 (m, 18, PEt_3 CH_2's), 0.94−0.81 (m, 27, PEt_3 CH_3's).

^{13}C{^{1}H} NMR (acetone-d_6, 22 °C): δ 167.6 (quartet, J_{C-P} = 28.1 Hz, C1/C5), 132.0 (br s, C2/C4), 129.9 (quartet, J_{C-P} = 5.3 Hz, C3), 28.4 (quartet, J_{C-P} = 3.2 Hz, ring CH_3's), 22.7−22.1 (m, PEt_3 CH_2's), 9.2 (s, PEt_3 CH_3's).

^{31}P{^{1}H} NMR (acetone-d_6, 22 °C): δ −4.8 (s).

Synthesis of $\overline{CH{=}C(Me)CH{=}C(Me)CH{=}}Ir(PEt_3)_2(PMe_3)$ (4a). PMe_3 (1.44 g, 1.9×10^{-2} mol) was added to a solution of compound **3** (0.60 g, 0.94×10^{-3} mol) in diethyl ether. After stirring at room temperature for 12 h, the solvent was removed *in vacuo*. The residue was then redissolved in a minimal quantity of acetone and cooled to −30 °C, causing compound **4a** to crystallize. Yield: 0.40 g, 71%. Anal. Calcd for $C_{22}H_{48}IrP_3$: C, 44.20; H, 8.11. Found: C, 43.74; H, 7.85.

^{1}H NMR (acetone-d_6, 22 °C): δ 10.85 (d of t of d, J_{H-PMe_3} = 14.8 Hz, J_{H-PEt_3} = 4.1 Hz, J_{H-H} = 2.0 Hz, 2, H1/H5), 7.14 (br s, 1, H3), 2.50 (s, 6, ring CH_3's), 1.89−1.70 (m, 12, PEt_3 CH_2's), 1.66 (d, J_{H-P} = 7.3 Hz, 9, PMe_3 CH_3's), 0.91−0.77 (m, 18, PEt_3 CH_3's).

^{13}C{^{1}H} NMR (acetone-d_6, 22 °C): δ 167.9 (d of t, J_{C-PMe_3} = 33.5 Hz, J_{C-PEt_3} = 26.3 Hz, C1/C5), 132.5 (br s, C2/C4), 129.7 (t, J_{C-P} = 7.3 Hz, C3), 28.3 (br s, ring CH_3's), 23.4−22.6 (m, PMe_3 CH_3's and PEt_3 CH_2's), 9.0 (s, PEt_3 CH_3's).

^{31}P{^{1}H} NMR (acetone-d_6, 22 °C): δ 1.3 (d, J_{P-P} = 10.9 Hz, 2, PEt_3's), −44.3 (t, J_{P-P} = 10.9 Hz, 1, PMe_3).

Synthesis of $\overline{CH{=}C(Me)CH{=}C(Me)CH{=}}Ir(PEt_3)_2[P(OMe)_3]$ (4b). $P(OMe)_3$ (1.64 g, 1.32×10^{-2} mol) was added to a solution of compound **3** (0.42 g, 0.66×10^{-3} mol) in tetrahydrofuran. After the solution was stirred at room temperature for 20 h, the solvent was removed *in vacuo*. The residue was then redissolved in a minimal quantity of acetone, and the solution was cooled to −30 °C overnight, causing compound **4b** to crystallize. Yield: 0.30 g, 71%. Anal. Calcd for $C_{22}H_{48}IrO_3P_3$: C, 40.91; H, 7.51. Found: C, 40.95; H, 7.52.

^{1}H NMR (acetone-d_6, 22 °C): δ 11.05 (d of t of d, $J_{H-P(OMe)_3}$ = 11.8 Hz, J_{H-PEt_3} = 5.2 Hz, J_{H-H} = 1.8 Hz, 2, H1/H5), 7.22 (br s, 1, H3), 3.49 (d, J_{H-P} = 10.9 Hz, 9, $P(OMe)_3$ CH_3's), 2.52 (s, 6, ring CH_3's), 1.92−1.71 (m, 12, PEt_3 CH_2's), 0.88−0.73 (m, 18, PEt_3 CH_3's).

^{13}C{^{1}H} NMR (acetone-d_6, 22 °C): δ 169.4 (d of t, $J_{C-P(OMe)_3}$ = 52.1 Hz, J_{C-PEt_3} = 25.1 Hz, C1/C5), 133.5 (br s, C2/C4), 131.1 (quartet, J_{C-P} = 6.3 Hz, C3), 52.9 (d, J_{C-P} = 7.0 Hz, $P(OMe)_3$ CH_3's), 28.3 (br s, ring CH_3's), 21.9 (filled-in d, J_{C-P} = 28.2 Hz, PEt_3 CH_2's), 8.6 (s, PEt_3 CH_3's).

^{31}P{^{1}H} NMR (acetone-d_6, 22 °C): 123.1 (t, J_{P-P} = 31.0 Hz, 1, $P(OMe)_3$), 2.0 (d, J_{P-P} = 31.0 Hz, 2, PEt_3's).

Synthesis of $\overline{CH{=}C(Me)CH{=}C(Me)CH{=}}Ir(PEt_3)_2(CO)$ (4c). A stream of carbon monoxide at 1 atm pressure was bubbled through a refluxing acetone solution of compound **3** (0.32 g, 0.50×10^{-3} mol) for 30 min. After removal of the acetone solvent under vacuum, the residue was extracted with pentane and the extract filtered. NMR analysis of this extract showed **4c** to be the principal product, along with a small quantity of compound **7**.

^{1}H NMR (acetone-d_6, 22 °C): δ 11.26 (t of d, J_{H-P} = 3.7 Hz, J_{H-H} = 1.9 Hz, 2, H1/H5), 7.37 (br s, 1, H3), 2.50 (s, 6, ring CH_3's), 1.90−1.70 (m, 12, PEt_3 CH_2's), 0.97−0.80 (m, 18, PEt_3 CH_3's).

^{13}C{^{1}H} NMR (acetone-d_6, 22 °C): δ 192.3 (t, J_{C-P} = 6.0 Hz, CO), 171.6 (t, J_{C-P} = 23.0 Hz, C1/C5), 135.2 (t, J_{C-P} = 7.7 Hz, C3), 134.7 (t, J_{C-P} = 4.5 Hz, C2/C4), 27.8 (t, J_{C-P} = 3.1 Hz, ring CH_3's), 22.3 (filled-in d, J_{C-P} = 30.4 Hz, PEt_3 CH_2's), 8.5 (s, PEt_3 CH_3's).

^{31}P{^{1}H} NMR (acetone-d_6, 22 °C): δ 4.0 (s).

Synthesis of $\overline{CH{=}C(Me)CH{=}C(Me)CH{=}}Ir(PEt_3)(PMe_3)_2$ (5a). PMe_3 (0.038 g, 5.0×10^{-4} mol) was added to a solution of compound **3** (0.15 g, 2.3×10^{-4} mol) in toluene. After the solution was heated at reflux for 1 h, the solvent was removed *in vacuo*. The residue was extracted with pentane and the extract filtered. NMR analysis of this crude extract showed **5a** to be the principal product, along with smaller quanties of **4a** and **6**.

^{1}H NMR (acetone-d_6, 22 °C): δ 10.76 (t, J_{H-PMe_3} = 12.6 Hz, 2, H1/H5), 7.12 (m, 1, H3), 2.50 (s, 6, ring CH_3's), 1.64 (d, J_{H-P} = 7.3 Hz, 18, PMe_3 CH_3's), 1.64−1.54 (m, 6, PEt_3 CH_2's), 0.81−0.69 (m, 9, PEt_3 CH_3's).

^{13}C{^{1}H} NMR (acetone-d_6, 22 °C): δ 167.8 (t of d, J_{C-PMe_3} = 32.7 Hz, J_{C-PEt_3} = 22.9 Hz, C1/C5), 132.7 (d, J_{C-P} = 7.7 Hz, C2/C4), 129.7 (d of t, J_{C-PEt_3} = 10.8 Hz, J_{C-PMe_3} = 2.8 Hz, C3), 28.4 (br s, ring CH_3's), 23.7−23.0 (complex m, PMe_3 CH_3's and PEt_3 CH_2's), 8.6 (s, PEt_3 CH_3's).

^{31}P{^{1}H} NMR (acetone-d_6, 22 °C): δ 10.2 (t, J_{P-P} = 14.5 Hz, 1, PEt_3), −42.1 (d, J_{P-P} = 14.5 Hz, 2, PMe_3's).

Synthesis of $\overline{CH{=}C(Me)CH{=}C(Me)CH{=}}Ir(PEt_3)[P(OMe)_3]_2$ (5b). $P(OMe)_3$ (0.70 g, 5.6×10^{-3} mol) was added to a solution of compound **3** (0.090 g, 1.4×10^{-4} mol) in toluene. After the solution was heated at reflux for 30 min, the solvent was removed *in vacuo*. The residue was extracted with pentane and the extract filtered. After removal of the pentane solvent, the residue was dissolved in a minimal quantity of acetone, and this solution was cooled to −30 °C, producing yellow crystals of **5b**. Yield: 0.068 g (75%). Anal. Calcd for $C_{19}H_{42}IrO_6P_3$: C, 35.01; H, 6.51. Found: C, 35.12; H, 6.40.

^1H NMR (benzene-d_6, 22 °C): δ 11.55 (t of d of d, $J_{H-P(OMe)_3}$ = 8.9 Hz, J_{H-PEt_3} = 3.7 Hz, J_{H-H} = 1.9 Hz, 2, H1/H5), 7.89 (br s, 1, H3), 3.27 (filled-in d, J_{H-P} = 11.3 Hz, 18, $P(OMe)_3$ CH_3's), 3.04 (s, 6, ring CH_3's), 1.95−1.85 (m, 6, PEt_3 CH_2's), 0.85−0.75 (m, 9, PEt_3 CH_3's).

$^{13}C\{^1H\}$ (benzene-d_6, 22 °C): δ 169.2 (t of d, $J_{C-P(OMe)_3}$ = 45.5 Hz, J_{C-PEt_3} = 22.7 Hz, C1/C5), 135.1 (q, J_{C-P} = 4.0 Hz, C2/C4), 133.1 (q, J_{C-P} = 7.0 Hz, C3), 51.8 (s, $P(OMe)_3$ CH_3's), 28.5 (br t, J_{C-P} = 5.4 Hz, ring CH_3's), 21.2 (d, J_{C-P} = 27.3 Hz, PEt_3 CH_2's), 8.0 (s, PEt_3 CH_3's).

$^{31}P\{^1H\}$ NMR (benzene-d_6, 22 °C): δ 130.5 (d, J_{P-P} = 32.0 Hz, 2, $P(OMe)_3$'s), 6.8 (t, J_{P-P} = 32.0 Hz, 1, PEt_3).

Synthesis of $\overline{CH{=}C(Me)CH{=}C(Me)CH{=}}Ir(PMe_3)_3$ (6). PMe_3 (0.57 g, 7.5×10^{-3} mol) was added to a solution of compound **3** (0.24 g, 3.8×10^{-4} mol) in toluene. After the solution was heated at reflux for 1 h, the solvent was removed *in vacuo*. The residue was extracted with pentane and the extract filtered. After removal of the pentane solvent, the residue was dissolved in a minimal quantity of acetone and cooled to −30 °C, producing orange crystals of **6**. Yield: 0.15 g (75%). Anal. Calcd for $C_{16}H_{36}IrP_3$: C, 37.41; H, 7.08. Found: C, 37.11; H, 6.92.

^1H NMR (acetone-d_6, 22 °C): δ 10.62 (quartet of d, J_{H-P} = 8.0 Hz, J_{H-H} = 1.4 Hz, 2, H1/H5), 7.10 (br s, 1, H3), 2.50 (s, 6, ring CH_3's), 1.55 (filled-in d, J_{H-P} = 8.2 Hz, 27, PMe_3 CH_3's).

$^{13}C\{^1H\}$ NMR (acetone-d_6, 22 °C): δ 167.9 (quartet, J_{C-P} = 30.1 Hz, C1/C5), 133.1 (br s, C2/C4), 129.1 (quartet, J_{C-P} = 5.2 Hz, C3), 28.4 (q, J_{C-P} = 3.5 Hz, ring CH_3's), 23.8−23.0 (m, PMe_3 CH_3's).

$^{31}P\{^1H\}$ NMR (acetone-d_6, 22 °C): δ −36.1 (s, PMe_3's).

Synthesis of *trans*-(3,5-dimethylphenoxy)$Ir(PEt_3)_2(CO)$ (7). A stream of carbon monoxide (1 atm) was bubbled through a refluxing toluene solution of compound **3** (0.31 g, 4.8×10^{-4} mol) for 30 min. After removal of the toluene solvent, the residue was extracted with pentane and the extract filtered. Removal to the pentane solvent, followed by addition of minimal acetone and cooling to −30 °C, caused **7** to crystallize overnight. Yield: 0.27 g (98%). Anal. Calcd for $C_{21}H_{39}IrO_2P_2$: C, 43.65; H, 6.82. Found: C, 43.11; H, 7.13.

^1H NMR (benzene-d_6, 22 °C): δ 6.76 (s, 2, ortho H's), 6.34 (s, 1, para H), 2.26 (s, 6, ring CH_3's), 1.65−1.55 (m, 12, PEt_3 CH_2's), 1.03−0.92 (m, 18, PEt_3 CH_3's).

$^{13}C\{^1H\}$ (benzene-d_6, 22 °C): δ 176.0 (t, J_{C-P} = 10.4 Hz, CO), 169.8 (s, ipso C), 137.8 (s, meta C's), 118.6 (s, ortho C's), 116.9 (s, para C), 21.8 (s, ring CH_3's), 17.0 (virtual t, J_{C-P} = 30.8 Hz, PEt_3 CH_2's), 8.3 (s, PEt_3 CH_3's).

$^{31}P\{^1H\}$ NMR (benzene-d_6, 22 °C): δ 23.7 (s, PEt_3's).

Reaction of $\overline{CH{=}C(Me)CH{=}C(Me)CH{=}}Ir(PEt_3)_3$ (3) with H_2. At room temperature, compound **3** in benzene-d_6 was treated with excess H_2 gas at 1 atm of pressure for 24 h. The color of the solution gradually changed from red to light yellow. The volatile fraction was removed under vacuum and analyzed by NMR. The principal organic products were 2,4-dimethyl-1-pentene and 2,4-dimethyl-1,3-pentadiene. The residue was also analyzed by NMR and shown to contain primarily $(H)_5Ir(PEt_3)_2$, together with smaller quantities of *mer*- and *fac*-$(H)_3Ir(PEt_3)_3$.

Synthesis of $\overline{CH{=}C(Me)CH{=}C(Me)CH{=}}Ir(PEt_3)_2(I)_2$ (8a). I_2 (0.16 g, 0.63×10^{-3} mol) was added to a cold (−30 °C), stirred solution of compound **3** (0.40 g, 0.63×10^{-3} mol) in acetone. The reaction solution was then warmed to room temperature and stirred for 30 min. During this time, the color of the solution changed from red to dark yellow-green. After removal of the solvent under vacuum, the residue was redissolved in a minimal quantity of acetone and the solution was cooled to −30 °C overnight, producing dark yellow-green crystals of compound **8a**. Yield: 0.41 g, 85%. Anal. Calcd for $C_{19}H_{39}I_2IrP_2$: C, 29.42; H, 5.08. Found: C, 29.82; H, 5.28.

^1H NMR (acetone-d_6, 22 °C): δ 13.95 (s, 2, H1/H5), 7.86 (s, 1, H3), 2.37 (s, 6, ring CH_3's), 2.12−1.90 (m, 12, PEt_3 CH_2's), 1.00−0.78 (m, 18, PEt_3 CH_3's).

$^{13}C\{^1H\}$ NMR (acetone-d_6, 22 °C): δ 215.1 (s, C1/C5), 161.6 (s, C3), 134.8 (s, C2/C4), 25.4 (s, ring CH_3's), 19.34 (virtual t, J_{C-P} = 36.4 Hz, PEt_3 CH_2's), 8.62 (s, PEt_3 CH_3's).

$^{31}P\{^1H\}$ NMR (acetone-d_6, 22 °C): δ −22.6 (s).

Synthesis of $\overline{CH{=}C(Me)CH{=}C(Me)CH{=}}Ir(PEt_3)_2(Br)_2$ (8b). Br_2 (0.19 g, 1.2×10^{-3} mol) was added dropwise to a cold (−78 °C), stirred solution of compound **3** (0.75 g, 1.2×10^{-3} mol) in acetone. The reaction solution was then warmed to room temperature and stirred for 30 min. During this time, the color of the solution changed from red to dark blue. After removal of the solvent under vacuum, the residue was redissolved in a minimal quantity of acetone and the solution was cooled to −30 °C overnight, producing dark blue crystals of compound **8b**. Yield: 0.70 g, 85%. Anal. Calcd for $C_{19}H_{39}Br_2IrP_2$: C, 33.48; H, 5.78. Found: C, 33.27; H, 5.87.

^1H NMR (acetone-d_6, 22 °C): δ 13.88 (s, 2, H1/H5), 7.89 (s, 1, H3), 2.43 (s, 6, ring CH_3's), 1.93−1.80 (m, 12, PEt_3 CH_2's), 0.99−0.84 (m, 18, PEt_3 CH_3's).

$^{13}C\{^1H\}$ NMR (acetone-d_6, 22 °C): δ 215.7 (s, C1/C5), 162.2 (s, C3), 134.4 (s, C2/C4), 25.3 (s, ring CH_3's), 16.3 (virtual t, J_{C-P} = 36.4 Hz, PEt_3 CH_2's), 7.7 (s, PEt_3 CH_3's).

$^{31}P\{^1H\}$ NMR (acetone-d_6, 22 °C): δ −8.2 (s).

Synthesis of $[\overline{CH{=}C(Me)CH{=}C(Me)CH{=}}Ir(PEt_3)_2(NCMe)_2]^{2+}(BF_4^-)_2$ (9). $AgBF_4$ (0.10 g, 5.2×10^{-4} mol) in 5 mL of acetonitrile was added slowly to a stirred solution of compound **3** (0.17 g, 2.6×10^{-4} mol) in 30 mL of acetonitrile. After it was stirred for several hours, the reaction mixture was filtered and the solvent was removed *in vacuo* to give an oily residue. This residue was redissolved in a minimal quantity of acetone, and pentane was added, causing **9** to precipitate as a blue spectroscopically pure product. Yield: 0.21 g, 95%.

^1H NMR (acetone-d_6, 22 °C): δ 13.02 (s, 2, H1/H5), 8.16 (s, 1, H3), 2.90 (s, 6, $NCCH_3$ CH_3's), 2.41 (s, 6, ring CH_3's), 1.86 (m, 12, PEt_3 CH_2's), 1.02 (m, 18, PEt_3 CH_3's).

$^{13}C\{^1H\}$ NMR (acetone-d_6, 22 °C): δ 210.8 (s, C1/C5), 172.3 (s, C3), 138.3 (s, C2/C4), 127.2 (s, N*C*CH$_3$), 24.7 (s, ring CH_3's), 15.1 (virtual t, J_{C-P} = 35.4 Hz, PEt_3 CH_2's), 7.1 (s, PEt_3 CH_3's), 3.7 (s, NC*C*H$_3$).

$^{31}P\{^1H\}$ NMR (acetone-d_6, 22 °C): δ 11.9 (s, PEt_3's).

Synthesis of $\overline{CH{=}C(Me)CHC(Me){=}CH}Ir(O{-}O)(PEt_3)_3$ (10). A stirred solution of compound **3** (0.35 g, 0.55×10^{-3} mol) in pentane was exposed to air for 15 min. During this time, the solution gradually turned from red to yellow. After removal of the solvent *in vacuo*, the residue was redissolved in a minimal quantity of diethyl ether and cooled to −30 °C, producing light yellow crystals of compound **10**. Yield: 0.29 g, 79%. Anal. Calcd for $C_{25}H_{54}IrO_2P_3$: C, 44.69; H, 8.12. Found: C, 44.85; H, 8.10.

^1H NMR (C_6D_6, 22 °C): δ 7.37 (m, 2, H1/H5), 4.59 (s, 1, H3), 2.32 (s, 6, ring CH_3's), 1.95−1.77 (m, 6, PEt_3 CH_2's), 1.71−1.53 (m, 12, PEt_3 CH_2's), 1.10−0.97 (m, 18, PEt_3 CH_3's), 0.82−0.69 (m, 9, PEt_3 CH_3's).

$^{13}C\{^1H\}$ NMR (C_6D_6, 22 °C): 132.1 (d of t, J_{C-P} = 89.4 Hz, 9.2 Hz, C1/C5), 129.5 (s, C2/C4), 92.3 (s, C3), 26.5 (t, J_{C-P} = 4.7 Hz, ring CH_3's), 19.8 (d, J_{C-P} = 32.2 Hz, PEt_3 CH_2's), 16.1 (d, J_{C-P} = 22.8 Hz, PEt_3 CH_2's), 8.7 (m, PEt_3 CH_3's).

$^{31}P\{^1H\}$ NMR (C_6D_6, 22 °C): δ −29.5 (t, J_{P-P} = 9.5 Hz, 1, PEt_3), −35.8 (d, J_{P-P} = 9.5 Hz, 2, PEt_3's).

Synthesis of $\overline{CH{=}C(Me)CHC(Me){=}CH}Ir[O{-}N(Ph)](PEt_3)_3$ (11). Nitrosobenzene (0.050 g, 4.7×10^{-4} mol) was

added to a cold (0 °C) solution of compound **3** (0.30 g, 4.7 × 10^{-4} mol) in tetrahydrofuran. The solution was stirred for 10 min before removing the tetrahydrofuran solvent under vacuum. The residue was dissolved in diethyl ether and the solution filtered. After the ether was removed, the residue was redissolved in a minimal amount of acetone and cooled to −30 °C overnight, producing yellow crystals of compound **11**. Yield: 0.23 g, 65%. Anal. Calcd for $C_{31}H_{59}IrNOP_3$: C, 49.84; H, 7.98. Found: C, 50.19; H, 8.02.

^{1}H NMR (toluene-d_8, −50 °C, stabilized with added PEt_3): δ 7.40−7.15 (m's, 6, H1/H5 and phenyl H's), 6.64 (br s, 1, phenyl H), 5.04 (s, 1 H3), 2.38 (s, 6, ring CH_3's), 1.88 (m, 6, PEt_3 CH_2's), 1.54 (m, 12, PEt_3 CH_2's), 0.90 (m, 18, PEt_3 CH_3's), 0.67 (m, 9, PEt_3 CH_3's).

^{31}P{^{1}H} NMR (toluene-d_8, −50 °C, stabilized with added PEt_3): −24.5 (t, J_{P-P} = 9.0 Hz, 1, PEt_3), −30.0 (d, J_{P-P} = 9.0 Hz, 2, PEt_3's).

Synthesis of CH=C(Me)CHC(Me)=CHIr[CHC(O)OC(O)CH](PEt$_3$)$_3$ (12). Maleic anhydride (0.032 g, 3.3 × 10^{-4} mol, dried in a desiccator before use) was added to a cold (−30 °C), stirred solution of compound **3** (0.21 g, 3.3 × 10^{-4} mol) in acetone. The solution was then stirred for 10 min and filtered. After removal of the acetone solvent under vacuum, the product was dissolved in a minimal amount of methylene chloride and cooled to −30 °C overnight, producing yellow crystals of compound **12**. Yield: 0.20 g, 80%. Anal. Calcd for $C_{29}H_{56}IrO_3P\cdot{}^1/_4CH_2Cl_2$: C, 46.27; H, 7.52. Found: C, 46.25; H, 7.45. See Figure 6 for the numbering scheme of H's and C's in the following spectra.

^{1}H NMR (methylene chloride-d_2, 22 °C): δ 6.71 (m, 2, H1 and H5), 3.41 (q of d, J = 9.6 Hz, 2.4 Hz, 1, H6), 3.24 (d, J = 4.0 Hz, 1, H3), 2.76 (m, 1, H9), 2.30−1.65 (m, 24, PEt_3 CH_2's and ring CH_3's), 1.20−0.85 (m, 27, PEt_3 CH_3's).

^{13}C{^{1}H} NMR (methylene chloride-d_2, 22 °C): 185.8 (s, C7 or C8), 177.2 (s, C7 or C8), 133.7 (s, C2 or C4), 132.3 (s, C2 or C4), 125.9 (d of t, J_{C-P} = 82.5 Hz, 8.7 Hz, C1 or C5), 124.3 (d of t, J_{C-P} = 82.8 Hz, 9.0 Hz, C1 or C5), 57.5 (s, C3), 46.9 (s, C9), 27.7 (d, J_{C-P} = 9.2 Hz, ring CH_3's), 25.3 (d, J_{C-P} = 9.6 Hz, ring CH_3's), 19.2 (d, J_{C-P} = 20.4 Hz, PEt_3 CH_2's), 18.6 (d, J_{C-P} = 28.4 Hz, PEt_3 CH_2's), 17.7 (d, J_{C-P} = 20.4 Hz, PEt_3 CH_2's), 9.7 (d, J_{C-P} = 4.8 Hz, PEt_3 CH_3's), 9.3 (d, J_{C-P} = 5.4 Hz, PEt_3 CH_3's), 9.0 (d, J_{C-P} = 5.9 Hz, PEt_3 CH_3's). The signal for C6 is obscured.

^{31}P{^{1}H} NMR (methylene chloride-d_2, 22 °C): δ −36.8 (t, J_{P-P} = 13.9 Hz, 1, PEt_3), −43.4 (t, J_{P-P} = 13.9 Hz, 1, PEt_3), −44.8 (t, J_{P-P} = 13.9 Hz, 1, PEt_3).

Synthesis of CH=C(Me)CHC(Me)=CHIr[S−C(S)](PEt$_3$)$_3$ (13). Carbon disulfide (0.36 g, 4.7 × 10^{-3} mol) was added to a cold (0 °C) solution of compound **3** (0.30 g, 4.7 × 10^{-4} mol) in tetrahydrofuran. The solution was stirred for several hours before removing the tetrahydrofuran solvent under vacuum. The residue was dissolved in diethyl ether and the solution filtered. The ether was removed, and the residue was redissolved in a minimal amount of acetone and cooled to −30 °C overnight, producing yellow crystals of compound **13**. Yield: 0.20 g, 60%. Anal. Calcd for $C_{26}H_{54}IrP_3S_2$: C, 43.61; H, 7.62. Found: C, 43.19; H, 7.80.

^{1}H NMR (acetone-d_6, 22 °C): δ 6.78 (br quartet, J_{H-P} = 7.5 Hz, 2, H1/H5), 4.58 (s, 1, H3), 2.1−1.9 (m, 18, PEt_3 CH_2's), 1.95 (s, 6, ring CH_3's), 1.15−0.95 (m, 27, PEt_3 CH_3's).

^{13}C{^{1}H} NMR (methylene chloride-d_2, 22 °C): δ 252.0 (s, CS_2), 133.3 (s, C2/C4), 126.8 (d of t, J_{C-P} = 80.7 Hz, 10.1 Hz, C1/C5), 89.7 (s, C3), 27.3 (s, ring CH_3's), 19.3 (d, J_{C-P} = 31.4 Hz, PEt_3 CH_2's), 19.1 (d, J_{C-P} = 25.5 Hz, PEt_3 CH_2's), 9.2 (s, PEt_3 CH_3's), 9.1 (s, PEt_3 CH_3's).

^{31}P{^{1}H} NMR (acetone-d_6, 22 °C): δ −30.0 (t, J_{P-P} = 15.6 Hz, 1, PEt_3), −38.1 (d, J_{P-P} = 15.6 Hz, 2, PEt_3's).

Synthesis of CH=C(Me)CHC(Me)=CHIr[S(O)$_2$](PEt$_3$)$_3$ (14). Sulfur dioxide was bubbled through a cold (0 °C) stirred solution of compound **3** (0.30 g, 4.7 × 10^{-4} mol) in tetrahydrofuran, causing the solution to rapidly lose its color. The tetrahydrofuran was removed under vacuum, and the residue was dissolved in diethyl ether and filtered. Following removal of the ether under vacuum, the product was redissolved in a minimal quantity of acetone and cooled to −30 °C overnight, producing colorless crystals of compound **14**. Yield: 0.21 g, 65%. Anal. Calcd for $C_{25}H_{54}IrO_2P_3S$: C, 42.65; H, 7.75. Found: C, 42.50; H, 7.77.

^{1}H NMR (acetone-d_6, 22 °C): 6.91 (br quartet, J_{H-P} = 6.3 Hz, 2, H1/H5), 3.83 (s, 1, H3), 2.23 (m, 6, PEt_3 CH_2's), 2.02 (s, 6, ring CH_3's), 2.00 (m, 12, PEt_3 CH_2's), 1.15 (m, 18, PEt_3 CH_3's), 0.98 (m, 9, PEt_3 CH_3's).

^{13}C{^{1}H} (acetone-d_6, 22 °C): δ 136.0 (s, C2/C4), 135.3 (d of t, J_{C-P} = 81.5 Hz, 9.5 Hz, C1/C5), 101.3 (s, C3), 22.8 (s, ring CH_3's), 19.8−19.0 (m's, PEt_3 CH_2's), 9.9 (s, PEt_3 CH_3's), 8.6 (d, J_{C-P} = 5.9 Hz, PEt_3 CH_3's).

^{31}P{^{1}H} NMR (acetone-d_6, 22 °C): δ −30.0 (t, J_{P-P} = 14.7 Hz, 1, PEt_3), −33.8 (d, J_{P-P} = 14.7 Hz, 2, PEt_3's).

Synthesis of CH=C(Me)CH=C(Me)CHIr[O−C(O)](PEt$_3$)$_3$ (15). Carbon dioxide was bubbled for 30 min through a stirred solution of compound **3** (0.30 g, 4.7 × 10^{-4} mol) in tetrahydrofuran. A slight pressure of CO_2 was then placed over the stirring solution for several hours. The tetrahydrofuran was removed, and the residue was dissolved in diethyl ether and filtered. The ether was removed, and the residue was dissolved in a minimal amount of acetone and cooled to −30 °C overnight, producing yellow crystals of compound **15**. Yield: 0.18 g, 55%. Anal. Calcd for $C_{26}H_{54}IrO_2P_3$: C, 45.66; H, 7.97. Found: C, 45.93: H, 7.89.

^{1}H NMR (acetone-d_6, 22 °C): δ 6.89 (dd, J_{H-P} = 16.0 Hz, 6.7 Hz, 1, H1), 5.49 (s, 1, H3), 3.17 (br d, J_{H-P} = 10.8 Hz, 1, H5), 2.15−1.75 (m's, 18, PEt_3 CH_2's), 2.02 (s, 3, ring CH_3's), 1.89 (s, 3, ring CH_3's), 1.20 (m, 18, PEt_3 CH_3's), 0.98 (m, 9, PEt_3 CH_3's).

^{13}C{^{1}H} NMR (acetone-d_6, 22 °C): δ 185.7 (s, CO_2), 135.6 (s, C2 or C4), 130.8 (s, C4 or C2), 128.1 (dd, J_{C-P} = 94.9 Hz, 11.6 Hz), 126.2 (s, C3), 29.1−28.7 (m's, ring CH_3's), 23.8 (d, J_{C-P} = 66.0 Hz, C5), 21.7 (d, J_{C-P} = 36.0 Hz, PEt_3 CH_2's), 17.6 (d, J_{C-P} = 20.5 Hz, PEt_3 CH_2's), 17.4 (d, J_{C-P} = 20.5 Hz, PEt_3 CH_2's), 9.8, 9.6, 9.1 (s's, PEt_3 CH_3's).

^{31}P{^{1}H} NMR (acetone-d_6, 22 °C): δ −28.4 (dd, J_{P-P} = 9.1 Hz, 3.6 Hz, 1, PEt_3), −28.8 (dd, J_{P-P} = 9.1 Hz, 3.6 Hz, 1, PEt_3), −32.1 (t, J_{P-P} = 9.1 Hz, 1, PEt_3).

Synthesis of CH=C(Me)CH=C(Me)Ir(PEt$_3$)$_2$(CO)(H) (16). Nitrous oxide was bubbled for 30 min through a stirred solution of compound **3** (0.49 g, 7.7 × 10^{-4} mol) in tetrahydrofuran. A slight pressure of N_2O was placed over the stirred solution for several hours. The tetrahydrofuran was removed and the residue was dissolved in pentane and filtered. The pentane was removed, resulting in a pure orange oil of compound **16**. Yield: 0.36 g, 88%.

^{1}H NMR (acetone-d_6, 22 °C): δ 7.32 (s, 1, H1), 6.38 (s, 1, H3), 2.32 (s, 3, ring CH_3), 1.88 (s, 3, ring CH_3), 2.0−1.5 (m, 12, PEt_3 CH_2's), 1.3−0.8 (m, 18, PEt_3 CH_3's), −10.6 (t, J_{H-P} = 18.0 Hz, 1, Ir−H).

^{13}C{^{1}H} NMR (acetone-d_6, 22 °C): δ 177.9 (t, J_{C-P} = 8.7 Hz, CO), 151.3 (t, J_{C-P} = 12.1 Hz, C4), 149.1 (s, C2), 147.2 (s, C3), 133.8 (t, J_{C-P} = 8.0 Hz, C1), 35.5 (s, ring CH_3), 22.6 (s, ring CH_3), 18.1 (virtual t, J_{C-P} = 35.8 Hz, PEt_3 CH_2's), 8.0 (s, PEt_3 CH_3's).

^{31}P{^{1}H} NMR (acetone-d_6, 22 °C): δ −9.1 (s, PEt_3's).

Synthesis of CH=C(Me)CH=C(Me)CH$_2$Ir[O=C(Me)-CH=C(Me)O](PEt$_3$)$_2$ (17). Excess 2,4-pentanedione was added to a stirred solution of compound **3** (0.21 g, 3.3 × 10^{-4} mol) in tetrahydrofuran at room temperature. Within 15 min, the color of the solution changed from red to deep yellow. After the tetrahydrofuran solvent was removed under vacuum, the residue was dissolved in diethyl ether and filtered. Following removal of the ether, the product was redissolved in a minimal

amount of acetone and cooled to −30 °C overnight, producing yellow crystals of **17**. Yield: 0.19 g, 92%. Anal. Calcd for $C_{24}H_{47}IrO_2P_2$: C, 46.35; H, 7.63. Found: C, 46.43; H, 7.86.

^{1}H NMR (benzene-d_6, 22 °C): δ 7.77 (s, 1, H1), 5.82 (s, 1, H3), 5.05 (s, 1, acac H), 3.44 (t, J_{H-P} = 13.0 Hz, H5's), 2.21 (s, 3, ring CH_3's), 2.07 (s, 3, ring CH_3's), 1.71 (s, 3, acac CH_3's), 1.70 (s, 3, acac CH_3's), 1.64 (m, 6, PEt_3 CH_2's), 1.59 (m, 6, PEt_3 CH_2's), 0.94 (m, 18, PEt_3 CH_3's).

^{13}C{^{1}H} NMR (benzene-d_6, 22 °C): δ 184.6 (s, acac CO), 184.2 (s, acac CO), 134.1 (s, C2 or C4), 130.7 (s, C3), 127.3 (t, J_{C-P} = 3.9 Hz, C2 or C4), 119.5 (t, J_{C-P} = 10.8 Hz, C1), 100.4 (s, acac CH), 28.5 (s, acac CH_3), 28.4 (s, acac CH_3), 27.9 (s, ring CH_3), 27.5 (s, ring CH_3), 12.5 (virtual t, J_{C-P} = 29.0 Hz, PEt_3 CH_2's), 7.3 (s, PEt_3 CH_3's), −9.3 (t, J_{C-P} = 6.8 Hz, C5).

^{31}P{^{1}H} NMR (benzene-d_6, 22 °C): δ −8.9 (s, PEt_3's).

Synthesis of CH=C(Me)CH=C(Me)CH$_2$Ir[O=C(OEt)-CH=C(OEt)O](PEt$_3$)$_2$ (18). Excess diethyl malonate was added to a stirred solution of compound **3** (0.25 g, 3.9 × 10^{-4} mol) in tetrahydrofuran at room temperature. Over a period of 2 h, the color of the solution changed from red to light orange. After removing the tetrahydrofuran solvent, the residue was dissolved in diethyl ether and filtered. Following removal of the ether, the product was redissolved in a minimal quantity of acetone and cooled to −30 °C overnight, causing **18** to crystallize as white needles: Yield: 0.22 g, 82%. Anal. Calcd for $C_{26}H_{51}IrO_4P_2$: C, 45.79; H, 7.56. Found: C, 45.66; H, 7.64.

^{1}H NMR (benzene-d_6, 22 °C): δ 7.67 (s, 1, H1), 5.77 (s, 1, H3), 4.79 (s, 1, malonate H), 4.12 (q, J_{H-H} = 7.2 Hz, 2, OEt CH_2's), 4.06 (q, J_{H-H} = 7.2 Hz, 2, OEt CH_2's), 3.45 (t, J_{H-P} = 13.1 Hz, 2, H5's), 2.17 (s, 3, ring CH_3's), 2.03 (s, 3, ring CH_3's), 1.69 (m, 6, PEt_3 CH_2's), 1.61 (m, 6, PEt_3 CH_2's), 1.13 (t, J_{H-H} = 7.2 Hz, 3, OEt CH_3's), 1.11 (t, J_{H-H} = 7.2 Hz, 3, OEt CH_3's), 0.95 (m, 18, PEt_3 CH_3's).

^{13}C{^{1}H} NMR (benzene-d_6, 22 °C): δ 173.3 (s, malonate CO), 173.2 (s, malonate CO), 133.8 (s, C2 or C4), 130.6 (s, C3), 126.5 (s, C2 or C4), 117.8 (t, J_{C-P} = 11.1 Hz, C1), 66.6 (s, malonate CH), 58.8 (s, OEt CH_2), 58.6 (s, OEt CH_2), 27.5 (s, ring CH_3), 27.2 (s, ring CH_3), 15.1 (s, OEt CH_3), 15.0 (s, OEt CH_3), 12.2 (virtual t, J_{C-P} = 29.1 Hz, PEt_3 CH_2's), 7.4 (s, PEt_3 CH_3's), -9.8 (t, J_{C-P} = 6.3 Hz, C5).

^{31}P{^{1}H} NMR (benzene-d_6, 22 °C): δ −7.9 (s, PEt_3's).

Synthesis of [(η^5-2,4-dimethylpentadienyl)Ir(PEt$_3$)$_3$]$^{2+}$-(O$_3$SCF$_3^-$)$_2$ (19). HO_3SCF_3 (0.10 g, 6.7 × 10^{-4} mol) was added to a cold (−30 °C) stirred solution of compound **3** (0.20 g, 3.1 × 10^{-4} mol) in acetone, causing the solution to rapidly lose its color. After 4 h at −30 °C, the acetone solvent was removed under vacuum and the residue was redissolved in a minimal quantity of acetone at room temperature. Diethyl ether was added until the solution became cloudy. The solution was then stored at −30 °C overnight, producing white crystals of **19**. Yield: 0.14 g, 48%. Anal. Calcd for $C_{27}H_{56}F_6IrO_6P_3S_2$: C, 34.49; H, 6.02. Found: C, 34.06; H, 6.25.

^{1}H NMR (acetone-d_6, 22 °C): δ 7.29 (s, 1, H3), 3.83 (br s, 2, $H1_{outer}$'s), 2.76 (s, 6, pentadienyl CH_3's), 2.54, 2.33, 2.06 (m's, 18, PEt_3 CH_2's), 2.41 (m, 2, $H1_{inner}$'s), 1.38−1.18 (m, 27, PEt_3 CH_3's).

^{13}C{^{1}H} (acetone-d_6, 22 °C): δ 142.7 (s, C2/C4), 94.6 (d, J_{C-P} = 9.5 Hz, C3), 50.1 (m, C1/C5), 25.5 (s, pentadienyl CH_3's), 24.0 (d, J_{C-P} = 35.0 Hz, PEt_3 CH_2's), 21.1 (br m, PEt_3 CH_2's), 10.5 (br s, PEt_3 CH_3's), 9.9 (d, J_{C-P} = 7.1 Hz, PEt_3 CH_3's).

^{31}P{^{1}H} NMR (acetone-d_6, 22 °C): δ −23.0 (t, J_{P-P} = 8.6 Hz, 1, PEt_3 under pentadienyl mouth), −32.4 (d, J_{P-P} = 8.6 Hz, 2, PEt_3's under pentadienyl chain).

Synthesis of [(η^6-1-fluoro-3,5-dimethyl-1-borabenzene)-Ir(PEt$_3$)$_3$]$^{2+}$(BF$_4^-$)$_2$ (20). Boron trifluoride was bubbled slowly through a cold (−78 °C) solution of compound **3** (0.16 g, 2.5 × 10^{-4} mol) in pentane. After several minutes, the solution decolorized and an off-white solid precipitated. The pentane solvent was removed under vacuum, and the solid was redissolved in acetone. After the mixture was stirred at room temperature for several hours, the volume of acetone was reduced, and the solution was cooled to −30 °C, causing **20** to crystallize as colorless blocks. Yield: 0.13 g (62%). Anal. Calcd for $C_{25}H_{54}B_3F_9IrP_3$: C, 35.60; H, 6.47. Found: C, 35.71; H, 6.81.

^{1}H NMR (acetone-d_6, 22 °C): δ 6.33 (s, 1, para H), 4.70 (s, 2, ortho H's), 2.69 (s, 6, ring CH_3's). 2.60−2.50 (m, PEt_3 CH_2's, 18), 1.45−1.30 (m, PEt_3 CH_3's, 27).

^{13}C{^{1}H} NMR (acetone-d_6, 22 °C): δ 152.1 (s, meta C's), 79.3 (s, para C), 78.3 (br s, ortho C's), 24.2 (br d, PEt_3 CH_2's), 23.9 (s, ring CH_3's), 11.5 (PEt_3 CH_3's).

^{31}P{^{1}H} NMR (acetone-d_6, −90 °C): δ −27.8 (d, J_{P-P} = 14.2 Hz, 2, PEt_3's), −29.8 (t, J_{P-P} = 14.2 Hz, 1, PEt_3).

Note: At room temperature, the ^{31}P NMR signal is a singlet due to a fluxional process (see text).

X-ray Diffraction Studies of CH=C(Me)CH=C(Me)-CH=Ir(PEt$_3$)$_3$ (3), CH=C(Me)CH=C(Me)CH=Ir(PMe$_3$)$_3$ (6), CH=C(Me)CH=C(Me)CH=Ir(PEt$_3$)$_2$(I)$_2$ (8a), CH=C-(Me)CHC(Me)=CHIr[CHC(O)OC(O)CH](PEt$_3$)$_3$ (12), CH=C(Me)CHC(Me)=CHIr[S(O)$_2$](PEt$_3$)$_3$ (14), and [(η^6-1-fluoro-3,5-dimethyl-1-borabenzene)Ir(PEt$_3$)$_3$]$^{2+}$(BF$_4^-$)$_2$ (20). Single crystals of compounds **3**, **6**, **8a**, **12**, **14**, and **20** were sealed in glass capillaries under an inert atmosphere. Data were collected at room temperature, using graphite-monochromated Mo Kα radiation. Three standard reflections were measured every 100 events as check reflections for crystal deterioration and/or misalignment.

All data reduction and refinement were done using the Siemens SHELXTL PLUS package on a VAX 3100 workstation.[58] Crystal data and details of data collection and structure analysis are listed in Table 1.

The iridium atom positions in compounds **3**, **6**, **8a**, **14**, and **20** were determined by direct methods; its position in compound **12** was calculated from a Patterson map. In all cases, remaining non-hydrogen atoms were found by successive full-matrix least-squares refinement and difference Fourier map calculations. In general, non-hydrogen atoms were refined anisotropically except in cases of disorder, while hydrogen atoms were placed at idealized positions and assumed the riding model.

Dynamic NMR Studies. Determination of $\Delta G^‡$ for Fluxional Processes Exhibited by Compounds 2 and 20. NMR spectra were recorded at 10 °C intervals over the temperature range where fluxional behavior was exhibited. Theoretical line shapes were calculated for a series of rates using the method of Johnson.[59,60] The experimental spectra were then matched against the theoretical spectra, and in this way, exchange rate constants were determined for each temperature. These exchange rate constants, k, were used to calculate the free energy of activation, $\Delta G^‡$, at each temperature, T, using the Eyring equation. The reported $\Delta G^‡$ is the average value over all of the temperatures in the simulation, and the uncertainty is the estimated standard deviation.

Kinetic Studies of the Conversion of CH=C(Me)-CH=C(Me)CH=Ir(PEt$_3$)$_3$ (3) to CH=C(Me)CH=C(Me)-CH=Ir(PEt$_3$)$_2$(PMe$_3$) (4a). In a typical kinetic run, compound **3** (1.6 × 10^{-2} g, 2.5 × 10^{-5} mol) and PMe_3 (1.9 × 10^{-2} g, 2.5 × 10^{-4} mol) were dissolved in 1 mL of acetone-d_6 in a 5 mm NMR tube, and a sealed glass capillary containing a ^{31}P NMR standard (neat PMe_2Ph) was added. The NMR probe

(58) Atomic scattering factors were obtained from the following: *International Tables for X-Ray Crystallography*; Kynoch Press: Birmingham, England, 1974; Vol. IV.

(59) Johnson, C. S., Jr. *Am. J. Phys.* **1967**, *35*, 929.

(60) Martin, M. L.; Martin, G. J.; Delpuech, J.-J. *Practical NMR Spectroscopy*; Heydon: London, 1980; pp 303−309.

Table 1. X-ray Diffraction Structure Summary

compd	**3**	**6**	**8a**	**12**	**14**	**20**
			Crystal Parameters and Data Collection Summary			
formula	$C_{25}H_{54}IrP_3$	$C_{16}H_{36}IrP_3$	$C_{19}H_{39}I_2IrP_2$	$C_{29}H_{56}IrO_3P_3{\cdot}CH_2Cl_2$	$C_{25}H_{54}IrO_2P_3S$	$C_{28}H_{60}B_3F_6IrOP_3$
fw	639.8	513.6	775.4	822.8	703.9	901.3
cryst syst	monoclinic	orthorhombic	orthorhombic	monoclinic	orthorhombic	triclinic
space group	$P2_1/n$	*Pbcm*	*Pbca*	*C*2/*c*	*Pnma*	$P\bar{1}$
a, Å	11.738(4)	7.630(2)	15.564(6)	19.122(3)	16.845(6)	11.198(2)
b, Å	15.643(3)	17.776(3)	20.913(6)	11.134(2)	17.850(6)	11.789(3)
c, Å	16.329(3)	16.119(4)	31.707(14)	34.110(6)	10.393(3)	16.405(4)
α, deg	90.0	90.0	90.0	90.0	90.0	109.52(2)
β, deg	95.81(2)	90.0	90.0	102.02(1)	90.0	90.10(2)
γ, deg	90.0	90.0	90.0	90.0	90.0	98.09(2)
V, Å^3	2982.9(13)	2197.1(9)	103 20(7)	7103(2)	3124.9(17)	2017.9(9)
Z	4	4	16	8	4	2
cryst dimens, mm	0.10 × 0.25 × 0.50	0.42 × 0.28 × 0.20	0.30 × 0.40 × 0.56	0.25 × 0.25 × 0.40	0.20 × 0.36 × 0.26	0.26 × 0.49 × 0.57
cryst color and habit	red plate	orange irregular	black prism	pale yellow prism	colorless cube	colorless prism
calcd density, g/cm^3	1.425	1.553	1.996	1.539	1.496	1.483
radiation, Å	Mo Kα, 0.710 73	Mo Kα, 0.710 73	Mo Kα, 0.710 73	Mo Kα, 0.710 73	Mo Kα, 0.710 73	Mo Kα, 0.710 73
scan type	$\theta-2\theta$	$\theta-2\theta$	ω	ω	$\theta-2\theta$	$\theta-2\theta$
scan rate, deg/min in ω	var; 2.44−14.65	var; 4.19−29.30	var; 4.88−14.65	var; 4.88−14.65	var; 2.49−14.65	var; 3.60−29.30
2θ range, deg	3.0−50.0	3.0−50.0	3.5−55.0	3.5−52.0	3.0−50.0	3.0−45.0
scan range (ω), deg	1.10 + Kα separation	1.20 + Kα separation	1.20	1.20	1.20 + Kα separation	1.20 + Kα separation
data collected	*h*, 0−13; *k*, 0−18; *l*, −19 to 19	*h*, −1 to 9; *k*, −21 to 1; *l*, −1 to 19	*h*, 0−20; *k*, 0−27; *l*, 0−41	*h*, −23 to 23; *k*, 0−13; *l*, 0−42	*h*, 0−20; *k*, 0−21; *l*, 0−12	*h*, 0−12; *k*, −12 to 12; *l*, −17 to 17
total decay	none detected	none detected	none detected	none detected	none detected	none detected
temp, K	295	295	295	295	296	295
			Treatment of Intensity Data and Refinement Summary			
no. of data collected	5774	2656	12822	7545	3127	5603
no. of unique data	5284	2019	11825	7035	2846	5281
no. of observed data	3680 with $I > 3\,\sigma(I)$	1600 with $I > 2\,\sigma(I)$	3321 with $I > 3\,\sigma(I)$	7031 with $I > 3\,\sigma(I)$	1872 with $I > 3\,\sigma(I)$	4816 with $I > 2\,\sigma(I)$
Mo Kα linear abs coeff, cm^{-1}	46.27	62.88	76.49	40.57	45.12	34.89
abs correction applied	semiempirical	semiempirical	semiempirical	semiempirical	semiempirical	semiempirical
data to param ratio	14.0:1	14.8:1	9.2:1	21.3:1	12.6:1	11.5:1
R^a	0.035	0.034	0.050	0.068	0.034	0.037
$R_w{}^a$	0.039[b]	0.074[c]	0.059[d]	0.057[e]	0.042[f]	0.053[g]
GOF[h]	1.34	1.02	1.20	1.17	1.00	1.83

[a] $R = \Sigma||F_o| - |F_c||/\Sigma|F_o|$. $R_w = [\Sigma w(|F_o| - |F_c|)^2/\Sigma w|F_o|^2]^{1/2}$. [b] $w = [\sigma^2(F_o) + 0.0003(F_o)^2]^{-1}$. [c] $w = [\sigma^2(F_o)^2 + (0.00468P)^2 + 0.9882P]^{-1}$ where $P = [(F_o)^2 + 2(F_c)^2]/3$. [d] $w = [\sigma^2(F_o) + 0.0010(F_o)^2]^{-1}$. [e] $w = [\sigma^2(F_o) + 0.0007(F_o)^2]^{-1}$. [f] $w = [\sigma^2(F_o) + 0.0009(F_o)^2]^{-1}$. [g] $w = [\sigma^2(F_o) + 0.0005(F_o)^2]^{-1}$. [h] GOF $= [\Sigma w(|F_o| - |F_c|)^2/(N_{observns} - N_{variables})]^{1/2}$.

was cooled or heated to the desired reaction temperature,[61] and ^{31}P NMR data were acquired at regular intervals (every 1 h at 15 °C, every 30 min at 25 °C, and every 10 min at 35 °C). The concentration of **3** was determined by integrating its ^{31}P NMR signal and scaling it to the integrated signal of the PMe_2Ph standard. Plots of ln([**3**]/[**3**]$_0$) versus time yielded straight lines from which first-order rate constants were extracted. An Eyring plot using first-order rate constants determined at 15, 25, and 35 °C yielded a straight line from which $\Delta H^{\ddagger}$ and $\Delta S^{\ddagger}$ were obtained.

Acknowledgment. Support from the National Science Foundation (Grant Nos. CHE-8520680, CHE-9003159, and CHE-9303516) and the donors of the Petroleum Research Fund, administered by the American Chemical Society, is gratefully acknowledged. We thank Johnson-Matthey Alfa/Aesar for a generous loan of $IrCl_3{\cdot}3H_2O$. Washington University's X-ray Crystallography Facility was funded by the National Science Foundation's Chemical Instrumentation Program (Grant No. CHE-8811456). Washington University's High Resolution NMR Service Facility was funded in part by National Institutes of Health Biomedical Support Instrument Grant 1 S10 RR02004 and by a gift from Monsanto Co. We thank Thomas Clayton, Jr., Laura Bass, Devran Boorsma, Shahid Murtuza, and Angela Wells for important contributions to this work.

(61) The NMR probe temperature was calibrated by using the temperature dependence of the frequency separation of the ^{1}H NMR resonances for the methyl and hydroxyl groups of neat methanol.

Supporting Information Available: Tables giving structure determination summaries and listings of final atomic coordinates, thermal parameters, bond lengths, and bond angles for compounds **3**, **6**, **8a**, **12**, **14**, and **20**, ORTEP drawings showing the positions of disordered atoms in **6**, **8a**, **12**, and **14**, a first-order kinetic plot for the conversion of **3** to **4a** at 25 °C, and an Eyring plot for the conversion of **3** to **4a** (57 pages). Ordering information is given on any current masthead page.

OM961012P